

KHIONE

User Manual

Version v8p5
December 1, 2023



Contents

1	Introduction	4
1.1	Positioning KHIONE within the ice modeling history	4
1.2	Overview of ice processes	5
1.3	Running a simulation with KHIONE	7
1.3.1	KHIONE's steering file	7
1.3.2	Activation of ice processes	7
1.3.3	Coupling with TELEMAT-2D	8
1.3.4	Managing tracers	8
1.3.5	Meteorological data	10
2	Heat budget	13
2.1	Surface heat exchange models	13
2.1.1	Linear Approximation	13
2.1.2	Comprehensive thermal budget formulation	14
2.2	Heat exchanges in presence of ice cover	15
2.3	Computation of heat fluxes	16
2.3.1	Solar radiation	16
2.3.2	Effective back radiation	18
2.3.3	Evaporative heat transfer	20
2.3.4	Conductive heat transfer	20
2.3.5	Heat exchanges due to precipitation	21
2.3.6	Heat exchange between water and ice cover	21
3	Supercooling and suspended frazil ice	24
3.1	Suspended Frazil Ice	24
3.1.1	Shape of frazil crystals	26
3.1.2	Thermal growth and melting	26
3.1.3	Secondary nucleation	29
3.1.4	Flocculation	31
3.1.5	Seeding	32
3.1.6	Deposition and erosion under the ice cover	33

3.2	Thermal balance	34
3.3	Salinity balance	35
3.4	Turbulence	36
3.5	Clogging or frazil accretion on racks	36
3.5.1	Inputs and outputs	37
3.5.2	Clogging on a set of vertical or horizontal bars	37
3.5.3	Clogging on a grid of vertical and horizontal bars	39
4	Ice cover	41
4.1	Introduction on ice cover processes	41
4.2	Dynamic ice cover	42
4.3	Static ice cover (border ice)	43
4.4	Thermal growth and decay of ice floes and ice cover	45
4.5	Mass exchange between suspended frazil ice and ice cover	47
4.6	Ice cover impact on hydrodynamics	48
4.6.1	Friction source term	48
4.6.2	Ice cover thickness gradient source term	50
	Bibliography	51

1. Introduction

KHIONE is a component of the TELEMAC SYSTEM, which focuses on modeling ice processes. It takes its name from the Greek goddess of snow and ice, daughter of Borea (the god of the cold northern wind), and who had a son with Poseidon (the god of the sea).

1.1 Positioning KHIONE within the ice modeling history

Numerical modelling studies have played an important role in river and coastal engineering, particularly so with ice modelling. The complexity of the formation and evolution of an ice sheet, as a result of heat exchanges at the air-ice-water interfaces, and its interaction with the underlying hydrodynamics, have restricted physical modelling studies to idealised experiments in flumes. Additionally, it is very difficult to scale ice structural dynamic processes such as accumulation of surface ice fragments in channels [23], [5].

Mathematical models can be a useful tool to investigate the numerous processes that interact in river systems under different flow, weather, and operational conditions. Thermal-ice processes have been considered in mathematical models with increasing complexity in the past couple of decades [43]. [24] developed a one-dimensional river ice model, RICE, which has been improved by [44], and [22]. The model is capable of simulating unsteady flow and ice processes in channel networks over a long winter period. Many river ice processes require two-dimensional analysis. A two-dimensional river ice dynamics model, DynaRICE, was developed by [45] and [26]. The hydrodynamic model includes the treatment of transcritical flows and wet-dry bed transitions. The DynaRICE models were extended to incorporate thermal-ice processes ([27], [43], [20]). Simulation of water temperature with super-cooling, frazil ice concentration, surface ice transport, ice cover progression, undercover ice transport, thermal growth and decay of ice covers, and ice-cover stability were included.

KHIONE was developed to allow the users to study ice related problems coupled with hydrodynamics. It was initially developed through a collaboration project between EDF R&D, HR Wallingford and Clarkson University and incorporated many components of the DynaRICE modeling software (like super-cooling and frazil ice) except for surface ice transport that was not fully integrated in KHIONE by then. Since this collaboration EDF R&D maintained the module, developed and integrated new models like the multi-class frazil ice model.

1.2 Overview of ice processes

Various ice processes can occur in cold regions during winter periods. These include complex interactions between thermal exchanges and ice dynamics coupled with hydrodynamics. The presence of ice in water affects the design and operation of coastal and riverine infrastructures and have an impact on ecological and environmental conditions of the river. An overview of the several ice processes that occur during a freeze-up period are presented in Figure 1.1 from the supercooling phase to the formation of an ice cover. The purpose of KHIONE is to allow the modeling of most of these processes taking advantage of the quality and reliability of the TELEMAC SYSTEM.

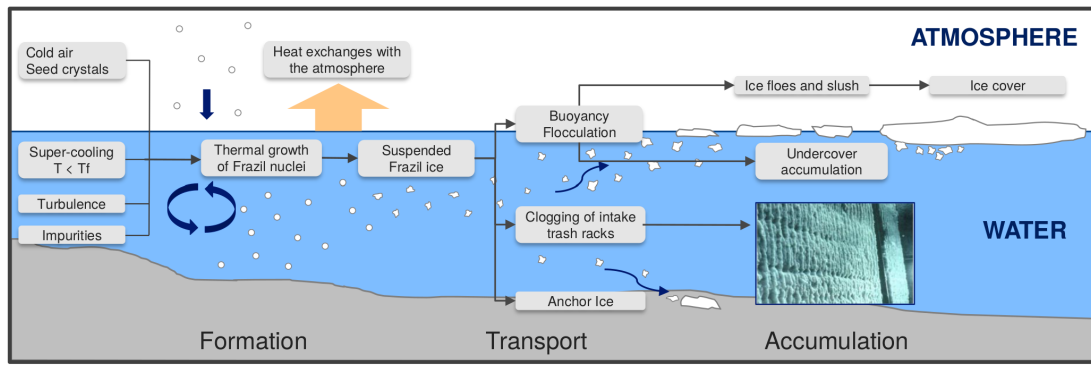


Figure 1.1: Overview of river ice processes

Suspended frazil ice is the primary form of ice in water bodies. Modeling suspended frazil ice formation requires a good understanding of the physical processes that leads to the apparition of nuclei and thermal growth of the crystals (see [11] and [12]). That includes heat exchanges between water and the atmosphere which is a key aspect to properly predict the cooling rate of water and the supercooling phase that lead to the thermal growth of frazil disks (a typical supercooling curve is presented in Figure 1.2).

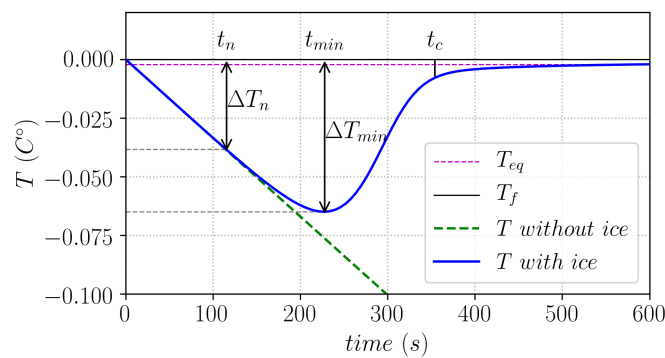


Figure 1.2: Typical supercooling curve with and without the formation of frazil ice.

Turbulence is another physical process that may have a significant impact on the frazil formation and thus needs to be modeled as well. Once frazil nuclei start to grow, the evolution of suspended ice in water bodies can lead to various ice types and forms depending on where and how it accumulates i.e. at the bottom of the water column (anchor ice) to the water surface (ice floes, slush and border ice) but also on submerged structures (clogging of trash racks). Subsequently surface ice can evolve into a thick ice cover if winter conditions are harsh enough. To ease the comprehension of the models included in KHIONE, it can be divided into several modules as shown in Figure 1.3 and presented hereafter.

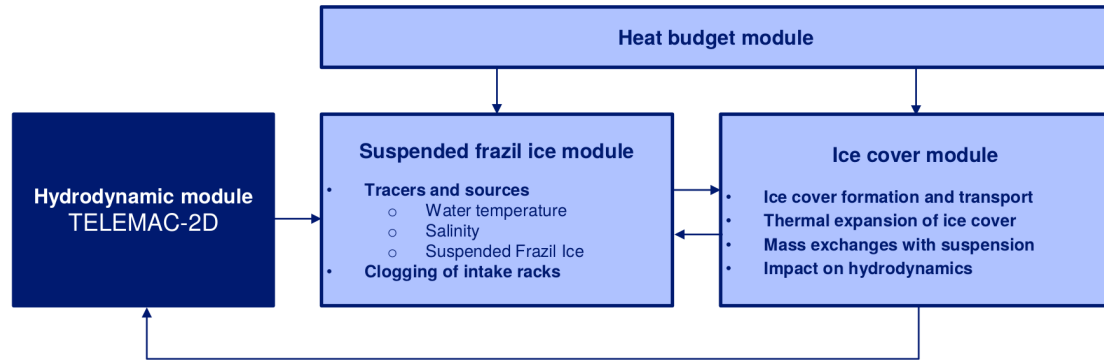


Figure 1.3: KHIONE modules

- ▷ A key component of KHIONE that both serve the frazil ice module and ice cover module is the heat budget module, presented in chapter 2. The module contains all the heat fluxes computations between the different media (atmosphere, water, ice cover) which includes the surface heat exchanges models as well as the heat exchange between the water column and the ice cover.
- ▷ The second and most advanced module of KHIONE deals with suspended frazil ice related processes. It consists in a set of advection-diffusion equations with source terms which allow the modeling of water temperature (supercooling), salinity and suspended frazil ice evolution. In practice KHIONE uses the tracer transport components of TELEMAC-2D and advection and diffusion operators are solved within the latter. Therefore only processes used to define each tracer source term are modeled within KHIONE. Balance equations and source terms for tracers are all presented in chapter 3. Besides suspended frazil ice can lead to clogging of submerged racks which can be modeled with KHIONE, see section 3.5 for more details.
- ▷ The last and more complex module deals with ice cover related models. It includes the formation and transport of ice cover as well as thermal expansion (or decay) of the ice cover. Additionally the mass exchanges with the suspended frazil ice and the impact on hydrodynamics is also taken into consideration. Ice cover related models are presented in the chapter 4.

Note:

The modeling of ice cover processes is still a work in progress in KHIONE. Ice cover dynamics is not yet fully implemented. The coupling with external ice cover models is advised for ice cover related applications.

1.3 Running a simulation with KHIONE

1.3.1 KHIONE's steering file

This file contains the necessary information for running a simulation with KHIONE, it also must include the values of parameters that are different from the default values (as specified in the dictionary file `khione.dico`):

- ▷ Input and output files
- ▷ Ice processes
- ▷ Physical and numerical parameters

Sketch of the KHIONE's steering file (*.cas)

```

/-----
/
/ Steering file for: KHIONE
/
/-----
/ FILES
/-----
/
GEOMETRY FILE           = 'geo_longflume.slf'
BOUNDARY CONDITIONS FILE = 'geo_longflume.cli'
/
/-----
/ ICE PROCESSES
/-----
/
HEAT BUDGET = YES
SALINITY = YES
BORDER ICE COVER = YES
CLOGGING ON BARS = YES
...
/-----
/ METEOROLOGY
/-----
/
ATMOSPHERE-WATER EXCHANGE MODEL = 1
...
/-----
/ FRAZIL ICE
/-----
/
NUMBER OF CLASSES FOR SUSPENDED FRAZIL ICE = 1
FRAZIL CRYSTALS RADIUS = 1.E-4
...

```

1.3.2 Activation of ice processes

Heat budget module

- ▷ When setting `HEAT BUDGET=YES` (default = YES) the heat exchanges with the atmosphere are activated (See chapter 2) as well as the heat exchanges between water and the ice cover. This is activated by default as the heat fluxes computations are required to describe the evolution of water temperature (and frazil ice) as well as the evolution of the ice cover thickness.

Suspended Frazil ice module

- ▷ When setting `HEAT BUDGET=YES` (default = YES) two tracers are defined, the first one being the water temperature, noted T and the second one being the suspended frazil ice

volume fraction, noted C (See chapter 3). Multiple classes of frazil can be selected, noted C_k , as described later on, in which case the number of tracer will be the number of frazil classes +1.

- ▷ If **SALINITY=YES** (default = NO) in the **KHIONE** steering file, one additional tracer is added to model salinity. This also affects the computation of the freezing temperature and include salt rejection effect due to frazil ice formation (See chapter 3). Consequently the tracers are water temperature (T), salinity (S) and frazil ice volume fractions (C_k) respectively.
- ▷ If **CLOGGING ON BARS=YES** (default = NO) in the frazil ice accumulation on trash racks is activated. See chapter 3 for additional details.

Ice cover module

- ▷ When setting **DYNAMIC ICE COVER=YES** (default = NO) a simple dynamic ice cover model is activated, which consists in two conservation equations on the ice cover surface fraction noted C_i and the ice cover thickness noted t_i (See chapter 4.2).
- ▷ When setting **BORDER ICE COVER=YES** (default = NO) a static border ice model is activated, in which the evolution of the ice cover thickness t_i is computed when a set of empirical formation criteria are met (See chapter 4.3).
- ▷ If **HEAT BUDGET=YES** (default = YES) the thermal expansion and decay of the ice cover is modeled depending on heat exchanges with the atmosphere (See chapter 4).
- ▷ The effect of ice cover on hydrodynamics can be set with **ICE COVER IMPACT ON HYDRODYNAMIC=YES** (default = NO) in which case the under cover friction as well as the surface ice pressure gradient effects are taken into account (See chapter 4).

1.3.3 Coupling with TELEMAT-2D

KHIONE, unlike other components of the **TELEMAT SYSTEM**, cannot be run in a stand-alone mode because ice processes are intertwined with hydrodynamic processes. Instead, a simulation using **KHIONE**, is carried out through **TELEMAT-2D** coupled with **KHIONE** and the **TELEMAT-2D** steering file should include **COUPLING WITH='KHIONE'** and the keyword **KHIONE STEERING FILE** to indicate the name of the **KHIONE** steering file:

```
...
/-----
/  COUPLING WITH KHIONE
/-----
/
COUPLING WITH          = 'KHIONE '
KHIONE STEERING FILE   = 'ice_frazil_growth.cas '
/
/ METEO DATA FILE (OPTIONAL)
ASCII ATMOSPHERIC DATA FILE = 't2d_frazil_growth_meteo.lqd'
/
...
```

1.3.4 Managing tracers

Depending on ice processes selected in the **KHIONE** steering file multiple tracers are included in the simulation (see section 1.3.2). Tracers are always stored in the same order, starting from **TEMPERATURE** followed by **SALINITY** and then by frazil volume fractions **FRAZIL k** where k is the class (frazil classes being stored from the lowest to the widest radius). If the number of class

is equal to 1, then the name of the frazil tracer is simply: FRAZIL. Last, the tracers representing the dynamic ice cover are listed: ICE COVER FRAC. and ICE COVER THICK..

Tracer initial and boundary conditions must be defined within the TELEMAC-2D or TELEMAC-3D steering file with as well as the associated numerical parameters for the TEMPERATURE and SALINITY tracers.

On the other hand, all ice related tracers are managed within the KHIONE steering file. The numerical tracers properties are set in the KHIONE steering file, with the following keywords:

- ▷ SCHEME FOR ADVECTION OF TRACERS, one value for all classes (default = 5),
 - 0 = no advection
 - 1 = characteristics
 - 2 = explicit SUPG
 - 3 = explicit Leo Postma
 - 4 = explicit MURD Scheme N
 - 5 = explicit MURD Scheme PSI
 - 13 = N-scheme for tidal flats LP
 - 14 = N-scheme for tidal flats
 - 15 = ERIA scheme only for 2D
- ▷ SCHEME OPTION FOR ADVECTION OF TRACERS, one value for all classes, only for PSI or N schemes (default = 4),
 - 1 = explicit
 - 2 = predictor-corrector
 - 3 = predictor-corrector second-order
 - 4 = implicit
- ▷ SCHEME FOR DIFFUSION OF FRAZIL IN 3D not used yet,
- ▷ SOLVER FOR DIFFUSION OF TRACERS, one value for all classes (default = 1),
 - 1: conjugate gradient,
 - 2: conjugate residual,
 - 3: conjugate gradient on a normal equation,
 - 4: minimum error,
 - 5: squared conjugate gradient,
 - 6: CGSTAB,
 - 7: GMRES,
 - 8: direct solver.
- ▷ SOLVER OPTION FOR DIFFUSION OF TRACERS, one value for all classes (default = 5),
- ▷ MAXIMUM NUMBER OF ITERATIONS FOR SOLVER FOR TRACERS, one value for all classes (default = 60),
- ▷ ACCURACY FOR DIFFUSION OF TRACERS, one value for all classes (default = 10^{-8}),

- ▷ PRECONDITIONING FOR DIFFUSION OF TRACERS, one value for all classes (default = 2),
 - 0: no preconditioning,
 - 2: diagonal,
 - 3: diagonal with the condensed matrix in 3D,
 - 5: diagonal with absolute values in 3D,
 - 7: Crout,
 - 11: Gauss-Seidel EBE in 3D,
 - 13: matrix defined by the user in 3D,
 - 14: diagonal and Crout,
 - 17: direct solver on the vertical in 3D,
 - 21: diagonal condensed and Crout in 3D,
 - 34: diagonal and direct solver on the vertical in 3D.
- ▷ COEFFICIENT FOR HORIZONTAL DIFFUSION OF FRAZIL not used yet,
- ▷ COEFFICIENT FOR VERTICAL DIFFUSION OF FRAZIL not used yet.

The physical properties of the tracers are then set individually in the KHIONE steering file, with the following keywords:

- ▷ INITIAL FRAZIL CONCENTRATION VALUES, one value by frazil class (default = 0 for all classes),
- ▷ PRESCRIBED FRAZIL CONCENTRATION VALUES, one value by frazil class and by liquid boundary, first set all prescribed values for the first boundary, then all values for the second, etc...,
- ▷ COEFFICIENT FOR DIFFUSION OF FRAZIL, one value by frazil class (default = 10^{-6} for all classes)
- ▷ INITIAL COVER CONCENTRATION VALUE (default = 0),
- ▷ PRESCRIBED COVER CONCENTRATION VALUES, one value by liquid boundary,
- ▷ COEFFICIENT FOR DIFFUSION OF COVER CONCENTRATION (default = 0),
- ▷ INITIAL THICKNESS CONCENTRATION VALUE (default = 0),
- ▷ PRESCRIBED THICKNESS CONCENTRATION VALUES, one value by liquid boundary,
- ▷ COEFFICIENT FOR DIFFUSION OF COVER THICKNESS (default = 0).

1.3.5 Meteorological data

Atmospheric drivers are a key part of any ice modeling study. There are two ways to provide atmospheric data to your simulations. If not provided via an ASCII ATMOSPHERIC DATA FILE, meteorological variables are considered constant during the simulation and can be defined in both the TELEMAT-2D steering file for the following keywords:

```

/-----
/  METEOROLOGY PARAMETERS (IN T2D)
/-----
/
AIR TEMPERATURE      = -10.0
CLOUD COVER          =  0.0
RAIN OR EVAPORATION  =  0.0
WIND VELOCITY ALONG X =  0.
WIND VELOCITY ALONG Y =  0.
/
...

```

and the KHIONE steering file for the following keywords:

```

/-----
/  METEOROLOGY PARAMETERS (IN KHIONE)
/-----
/
VISIBILITY            = 1000.0
DEWPOINT TEMPERATURE =  0.0
RELATIVE MODEL ELEVATION FROM MEAN SEA LEVEL = 0.
/
...

```

If provided in the TELEMAC-2D steering file with the keyword ASCII ATMOSPHERIC DATA FILE, the atmospheric data file should contain all the meteorological data required by the chosen atmosphere-water heat exchange model. If missing, the parameters are assumed to be constant with default values given by their keyword. An example of atmospheric data file is given below.

```

# Meteo File
#
# Columns order:
# TIME : Time (in seconds)
# TAIR : Air Temperature (in oC)
# WINDS: Wind Speed (m/s)
# CLDC : Cloud Cover (in tenths)
# PATM : Atmospheric Pressure (in Pa)
# RAIN : Rain (in m)
#
T      TAIR    CLDC    TDEW    VISBI    SNOW    RAINI    WINDS
s      degC   tenths  degree  km       mm/h    mm/h     m/s
0.     -10.    0.      0.      1000.    0       0        0.
3600.  -11.    1.      0.      1000.    0       0        0.
7200.  -9.     2.      0.      1000.    0       0        0.
10800. -8.     0.      0.      1000.    0       0        0.

```

One can note that the rain and the snow must be expressed as intensities, and not as cumulative values.

2. Heat budget

The thermal regime of the surface in contact with the atmosphere (water or ice) affects the surface ice evolution from freeze-up to breakup. This section describes heat fluxes or exchanges at the interface atmosphere - ice/water, as programmed within KHIONE.

2.1 Surface heat exchange models

There are two options provided to the user depending on the availability of atmospheric data: a comprehensive thermal budget (based on cloud cover, solar radiation, precipitation, winds, humidity, etc.) and a linearized formulation, the parameters of which should be calibrated. The model must be selected via the keyword `ATMOSPHERE-WATER EXCHANGE MODEL` (default = 0):

```
0 : LINEARISED FORMULA
1 : MODEL WITH COMPLETE BALANCE
```

2.1.1 Linear Approximation

The use of a simplified linearized formula has been popular in ice engineering since meteorological data necessary to compute full surface heat exchange may not be readily available. Since the diurnal variation of solar radiation and air temperature could be important to some of the ice processes such as frazil ice evolution, the linearized expression may include a component proportional to the difference between the surface temperature and the air temperature, and an independent short wave radiation component (Dingman and Assur 1969):

$$\phi = \phi_R + \alpha + \beta(T_a - T_s) \quad (2.1)$$

in which,

- ▷ ϕ is the total surface heat flux (from atmosphere to the surface), also noted ϕ_{aw} between air and water or ϕ_{ai} between air and ice (if there is ice cover)
- ▷ ϕ_R is the net short wave radiation,
- ▷ α a constant that can be set via the `WATER-AIR HEAT EXCHANGE CONSTANT` (default = -50 W.m^{-2}) in the case of water surface, or via `ICE-AIR HEAT EXCHANGE CONSTANT` (default = -32.547 W.m^{-2}) in case of ice surface,
- ▷ β a constant that can be set via the `WATER-AIR HEAT EXCHANGE COEFFICIENT` (default = $20 \text{ W.m}^{-2}.\text{K}^{-1}$) in the case of water surface, or via `ICE-AIR HEAT EXCHANGE COEFFICIENT` (default = $12.189 \text{ W.m}^{-2}.\text{K}^{-1}$) in case of ice surface,

- ▷ T_a is the air temperature,
- ▷ T_s is the surface temperature. If there is no ice cover, it is equal to the water temperature T_w otherwise it is equal to ice surface temperature.

2.1.2 Comprehensive thermal budget formulation

A dominating part of the heat exchanges occurs at the surface in contact with the atmosphere (air-water or air-ice interfaces) and includes short and long wave radiation, evaporation / condensation, sensible heat exchange, and precipitation [5], [35]. The total surface heat gain rate may be written as:

$$\phi = \phi_R + C_B\phi_B + C_E\phi_E + C_H\phi_H + C_P\phi_P \quad (2.2)$$

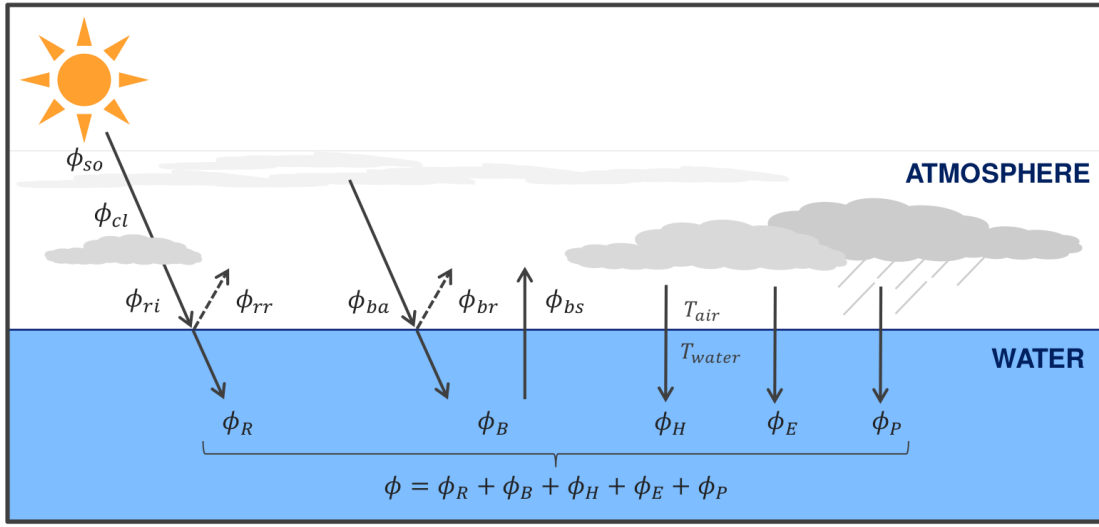


Figure 2.1: Comprehensive thermal budget formulation

in which,

- ▷ ϕ is the total surface heat flux (from atmosphere to the surface), also noted ϕ_{aw} between air and water or ϕ_{ai} between air and ice (if there is ice cover)
- ▷ ϕ_R is the net short wave radiation, which is the difference between the incoming solar radiation ϕ_{ri} and the solar radiation reflected back to the atmosphere ϕ_{rr} ,
- ▷ ϕ_B is the effective back radiation or terrestrial radiation, which is the net balance of the atmospheric long-wave radiation reaching the surface water ϕ_{ba} , the fraction of the atmospheric radiation reflected back by the surface water ϕ_{br} , and the long wave radiation emitted by the surface water ϕ_{bs} ,
- ▷ ϕ_E is the evaporation heat transfer,
- ▷ ϕ_H is the conductive or sensible heat transfer,
- ▷ ϕ_P is the heat transfer due to precipitation,
- ▷ C_B, C_E, C_H and C_P are calibration coefficient, with default values of 1, that can be adjusted via the following keywords:

COEFFICIENT FOR CALIBRATION OF BACK RADIATION
 COEFFICIENT FOR CALIBRATION OF EVAPORATIVE HEAT TRANSFERT
 COEFFICIENT FOR CALIBRATION OF CONDUCTIVE HEAT TRANSFERT
 COEFFICIENT FOR CALIBRATION OF PRECIPITATION HEAT TRANSFERT

Notes:

- ▷ The same convention is chosen for the sign of the fluxes ϕ_R to ϕ_P relative to the water body. Therefore a positive value means a heat gain (heat transfert from the atmosphere to water) and a negative value means a heat loss (heat release from water to the atmosphere).
- ▷ In WAQTEL with the THERMIC module, the short wave radiation is a user input as opposed to KHIONE in which it is computed from meteorological data.
- ▷ The conductive and evaporation heat transfer formulas in TELEMAC-2D are different from the ones used in KHIONE, which uses formulas that are more suitable for cold winter applications.

2.2 Heat exchanges in presence of ice cover

The total surface heat flux (from atmosphere to the surface) depends on the type of surface and therefore varies depending on whether there is ice cover or not. The heat flux ϕ is noted ϕ_{aw} between the atmosphere and water and ϕ_{ai} between the atmosphere and the ice cover. Additionally, when an ice cover is present, the heat exchange between water and the ice cover, noted ϕ_{wi} is modelled as well. A description of the heat exchanges in presence of ice cover is presented in Figure 2.2.

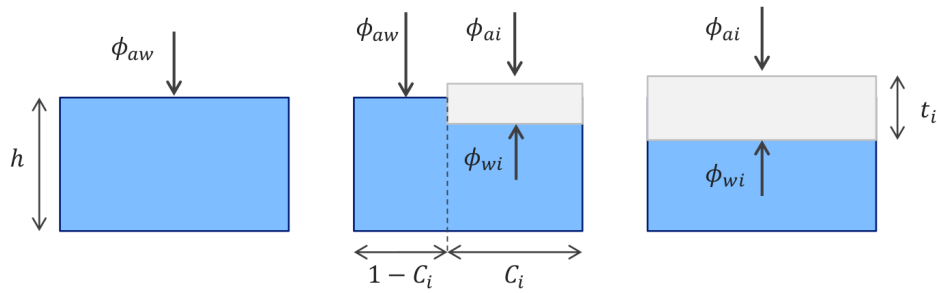


Figure 2.2: Heat exchanges description for open water (left) partially ice covered (middle) or fully ice covered water surface (right)

The ice cover is characterized by a thickness t_i and a surface fraction C_i , which both vary in space and time. The thickness evolution against time is a function of the heat fluxes on top and bottom of the ice sheet as presented in section 4.4. From the water perspective, when the water surface is fully covered, only the heat flux ϕ_{wi} is considered as opposed to the open water surface where only ϕ_{ai} affects water energy budget. In the case of a partially ice covered surface the heat flux affecting water temperature depends on C_i as described in Equation 3.24.

2.3 Computation of heat fluxes

The purpose of this section is to present how the heat fluxes are computed from ϕ_R (used in both atmosphere-water exchange models), to ϕ_B , ϕ_E , ϕ_H and ϕ_P (used only in the complete balance model).

2.3.1 Solar radiation

The net solar radiation ϕ_R is the difference between the incoming short wave radiation ϕ_{ri} (function of the radiation under clear skies ϕ_{cl} , and the cloud cover C [21]) and the short wave radiation reflected back to the atmosphere ϕ_{rr} when reaching water or ice surface. It can be expressed as follows:

$$\begin{aligned}\phi_R &= \phi_{ri} - \phi_{rr}, \\ \phi_{ri} &= \phi_{cl}(1 - 0.0065C^2), \\ \phi_{rr} &= R_t \phi_{ri},\end{aligned}\tag{2.3}$$

in which

- ▷ C is the cloud cover in tenths, with $C = 0$ for clear skies and $C = 10$ for overcast skies, which can be given in the TELEMAT-2D steering file by the keyword CLOUD COVER if not given in the meteo file. If the cloud cover data is not available, an estimated value might be used.
- ▷ R_t is the albedo or reflectivity, which varies from 6% to 10% for a water surface. The water albedo can be estimated as follows (Anderson 1954, [2]):

$$R_t = A\alpha^B\tag{2.4}$$

in which,

- ▷ α is the solar altitude in degrees,
- ▷ A and B are constants, depending on the amount of cloud cover, which can be computed by the following relationships ([8]):

$$\begin{aligned}A &= 2.20 + \frac{C_r^{0.7}}{4.0} - \frac{(C_r^{0.7} - 0.4)^2}{0.16} \\ B &= -1.02 + \frac{C_r^{0.7}}{16.0} + \frac{(C_r^{0.7} - 0.4)^2}{0.64}\end{aligned}\tag{2.5}$$

in which,

- ▷ $C_r = 1 - \phi_{ri}/\phi_{cl}$ is the cloudiness ratio, or the ratio of the difference between theoretical maximum solar radiation and the observed solar radiation, both for the same altitude of the sun, to the theoretical maximum solar radiation.

The ice albedo is directly set by the user with the keyword ALBEDO OF ICE (default = 0.2). [7] reported values for various ice conditions on the Great Lakes, North America, as summarized in the table below.

The incoming short wave radiation under clear skies, ϕ_{cl} , can be calculated as proposed by Iqbal (1983). ϕ_{cl} is computed as a function of the total extraterrestrial solar radiation per unit area incident on a horizontal surface ϕ_{so} , and the optical air mass m , as follows:

Table 2.1: Albedo of Great Lakes Ice ([7])

Ice type	Albedo (%)
Clear lake ice (snow free)	10
Bubbly lake ice (snow free)	22
Ball ice (snow free)	24
Refrozen Pancake (snow free)	31
Slush Curd (snow free)	32
Slush ice (snow free)	41
Brash ice (snow between blocks)	41
Snow ice (snow free)	46

$$\begin{aligned}
\phi_{cl} &= (0.99 - 0.17m)\phi_{so} \\
\phi_{so} &= \frac{12}{\pi} I_{so} E_0 \left[(\omega_1 - \omega_2) \sin \delta \cos \psi + (\sin \omega_1 - \sin \omega_2) \cos \delta \cos \psi \right] \\
m &= m_0 \frac{P_a}{P_0}
\end{aligned} \tag{2.6}$$

with

$$\begin{aligned}
m_0 &= \left[\sin \alpha_z + 0.15(\alpha_z + 3.885)^{-1.253} \right]^{-1} \\
\frac{P_a}{P_0} &= \exp(-0.0001184 z)
\end{aligned} \tag{2.7}$$

and

$$\begin{aligned}
\delta &= \frac{23.45\pi}{180} \sin \left[\frac{360}{365}(d_a + 284) \right] \\
E_0 &= 1 + 0.033 \cos \left(\frac{2\pi d_a}{365} \right) \\
\omega &= \frac{(12 - h)\pi}{12} \\
h &= t - \frac{\eta(L_{SM} - L_{LM})}{15} + E_t \\
E_t &= 3.8197(0.000075 + 0.001868 \cos r - 0.032077 \sin r - 0.014615 \cos 2r - 0.04089 \sin 2r) \\
r &= \frac{2\pi(d_a - 1)}{365}
\end{aligned} \tag{2.8}$$

in which,

- ▷ I_{so} is a solar constant, which is by default 1380 W/m^2 for the winter season and can be modified with the keyword `SOLAR CONSTANT`,
- ▷ d_a is the day number of the year from 1 to 365,
- ▷ E_0 is the eccentricity correction factor of the earth's orbit,
- ▷ h is the calculated hour and t is the current time in hour,
- ▷ η is the longitudinal orientation, -1 for west and $+1$ for east, which should be set with the keyword `EAST OR WEST LONGITUDE` (default = -1),
- ▷ L_{SM} is the global longitude from the standard meridian, set in the keyword `GLOBAL LONGITUDE, IN DEGREES` (default = 75),

- ▷ L_{LM} is the longitude in the local meridean, set in the keyword LOCAL LONGITUDE, IN DEGREES (default = 75.43),
- ▷ E_t is the equation of time,
- ▷ r is the difference between true and mean solar time,
- ▷ P_0 is the pressure at sea level,
- ▷ $\alpha_z = 90 - \theta_z$ is the solar latitude, with $\cos \theta_z = \sin \delta \sin \psi + \cos \delta \cos \psi \cos \omega$,
- ▷ ω is the hour angle in radians,
- ▷ δ is the solar declination, in radians,
- ▷ ψ is the latitude in degrees given by TELEMAC-W with the keyword LATITUDE OF ORIGIN POINT, north positive, south negative.

If KHIONE is coupled with TELEMAC-3D, the net solar radiation is applied in the entire water column. The penetration of the flux is represented with the equation:

$$S = \frac{1}{\rho C_p} \frac{\partial Q(z, \phi_R)}{\partial z}, \quad (2.9)$$

where the function $Q(z, \phi_R)$ is the residual solar radiation at the elevation z which writes:

$$Q(z, \phi_R) = \phi_R \exp(-K(z_s - z)), \quad (2.10)$$

with z_s the free surface elevation in m, and K the light extension coefficient in m^{-1} which can be set by the user through the keyword LIGHT EXTINCTION COEFFICIENT.

S is then treated as a source term in temperature advection-diffusion equation and writes:

$$S = \frac{\phi_R K \exp(-K(z_s - z))}{\rho C_p}. \quad (2.11)$$

2.3.2 Effective back radiation

The effective back radiation can be expressed as

$$\phi_B = \phi_{ba} - \phi_{br} - \phi_{bs} \quad (2.12)$$

in which,

- ▷ ϕ_{bs} is the long wave radiation from the water or ice surface,
- ▷ ϕ_{ba} is the atmospheric radiation,
- ▷ ϕ_{br} is the reflected long wave radiation.

Among all the heat exchange components, the long wave radiation from the surface has the largest magnitude. The Stefan-Boltzmann law gives

$$\phi_{bs} = \varepsilon_s \sigma T_{sk}^4 \quad (2.13)$$

in which,

- ▷ ϵ_s is the emissivity of the surface,
- ▷ σ is the Stefan-Boltzman constant, equal to $5.67 \times 10^{-8} \text{ W.m}^{-2}.\text{K}^{-4}$,
- ▷ T_{sk} is the surface temperature in the absolute scale (K).

The magnitude of the atmospheric radiation is generally larger than the net solar radiation reaching the ground, and is usually the second largest component among the various heat exchange processes. Under cloudy skies, the atmospheric radiation and the reflected long wave radiation can be computed by

$$\begin{aligned}\phi_{ba} &= \epsilon_a \sigma (1 + kC^2) T_{ak}^4 \\ \phi_{br} &= r_s \phi_{ba}\end{aligned}\tag{2.14}$$

in which,

- ▷ ϵ_a is the emissivity of the atmosphere,
- ▷ k is an empirical constant which depends on the cloud condition, typically about 0.0017,
- ▷ C is the cloud cover in tenth, already defined above
- ▷ $r_s = (1 - \epsilon_s)$ is the reflectivity of the surface, and
- ▷ T_{ak} is the air temperature at 2 m above the surface, in the absolute scale (K).

The emissivity of atmosphere can be estimated by [40]:

$$\begin{aligned}\epsilon_a &= 1.08 \left[1 - \exp \left(-e_a^{\left(\frac{T_{ak}}{106} \right)} \right) \right] \\ e_a &= \frac{R_H}{100} e_s\end{aligned}\tag{2.15}$$

in which,

- ▷ e_a is the vapor pressure in mbar,
- ▷ R_H is the relative humidity in percentage, and
- ▷ e_s is the saturated vapor pressure in mbar.

Vapor pressure can be determined by computing the saturated pressure at dew point. The Goff-Grath-Murray formula, [16], is used to compute saturated vapor pressure

- over water surface

$$\begin{aligned}e_s &= 7.95357242 \times 10^{10} \exp \left[-18.1972839 \frac{373.16}{T_{sk}} \right. \\ &\quad \left. + 5.02808 \ln \left(\frac{373.16}{T_{sk}} \right) - 20242.1852 \exp \left(\frac{-26.1205253}{373.16/T_{sk}} \right) \right. \\ &\quad \left. + 58.0691913 \exp \left(-8.039282 \frac{373.16}{T_{sk}} \right) \right]\end{aligned}\tag{2.16}$$

- over ice surface

$$e_s = 5.75185606 \times 10^{10} \exp \left[-20.947031 \frac{273.16}{T_{sk}} - 3.56654 \ln \left(\frac{273.16}{T_{sk}} \right) - \frac{2.01889049}{273.16/T_{sk}} \right] \quad (2.17)$$

in which,

▷ T_{sk} is the temperature in K

In summary, the effective back radiation, ϕ_B , is as follows:

$$\phi_B = -0.97\sigma \left[T_{sk}^4 - \epsilon_a(1 + kC^2)T_{ak}^4 \right] \quad (2.18)$$

2.3.3 Evaporative heat transfer

The heat transfer associated with evaporation or condensation, ϕ_E , when the vapor pressure in the air is greater than that at the surface, is given by the Rimsha-Donchenko 1957 formula, [38], as

$$\phi_E = -\frac{4.1855}{8.64} (1.56K_n + 6.08v_{a2})(e_{so} - e_a) \quad (2.19)$$

with

$$\begin{aligned} v_{a2} &= v_{az} \left(\frac{2}{z} \right)^{0.15} \\ K_n &= 8.0 + 0.35(T_s - T_a) \end{aligned} \quad (2.20)$$

in which,

- ▷ T_a is the air temperature in °C,
- ▷ T_s is the surface temperature (water or ice) in °C,
- ▷ e_{so} is the saturated vapor pressure corresponding to the surface temperature, in mbar,
- ▷ e_a is the vapor pressure corresponding to air temperature at 2 m above the surface, in mbar,
- ▷ v_{a2} is the wind velocity at 2 m above the surface.

2.3.4 Conductive heat transfer

The sensible heat transfer, ϕ_H , is proportional to the difference between the surface temperature and the air temperature, and is related to ϕ_E by the Bowen ratio. Based on the Rimsha-Donchenko formula above, ϕ_H is

$$\phi_H = \frac{4.1855}{8.64} (K_n + 3.9v_{a2})(T_{ak} - T_{sk}) \quad (2.21)$$

2.3.5 Heat exchanges due to precipitation

The heat transfert due to snow falling on the water surface, ϕ_P , can be estimated by

$$\phi_P = A_s \left[c_i(T_a - T_w) - L_i \right] \quad (2.22)$$

in which,

- ▷ A_s is the rate of snowfall over a unit area of surface in $\text{kg.m}^{-2}.\text{s}^{-1}$, equal to $(78.5/86400)\hat{V}^{-2.375}$ if snow is not given in the atmospheric data file.
- ▷ L_i is the latent heat of fusion of ice, equal to $3.3484 \times 10^5 \text{ J.kg}^{-1}$,
- ▷ c_i is the specific heat of ice, equal to $4.1855 \times 10^3 \text{ J.kg}^{-1}.\text{K}^{-1}$, and
- ▷ \hat{V} is the visibility in km.

When the precipitation is in the form of rainfall, the rate of heat gain can be calculated as

$$\phi_P = A_p c_p (T_a - T_w) \quad (2.23)$$

with

- ▷ A_p the rainfall rate,
- ▷ $c_p = 4.215 \times 10^3 \text{ J.kg}^{-1}.\text{K}^{-1}$ the specific heat of water.

The rainfall effect is generally small because the only contribution is the due to the specific heat effect associated with the difference in temperature between the water and the rain.

2.3.6 Heat exchange between water and ice cover

Similar to the thermal regime of the surface in contact with the atmosphere, the surface ice evolution from freeze-up to breakup depends also on the heat transfer under the cover. This section describes heat exchanges at the ice-water interface, as programmed within KHIONE. The heat transfer from water to ice under the surface ice, noted ϕ_{wi} , depends on the water temperature and flow condition, which may be expressed as

$$\phi_{wi} = h_{wi}(T_w - T_f) \quad (2.24)$$

in which,

- ▷ ϕ_{wi} is the heat flux between river water and ice,
- ▷ h_{wi} is a heat transfer coefficient, and
- ▷ T_f is the freezing point of water.

The heat transfer coefficient h_{wi} can be determined by formula for turbulent heat transfer in channels. Let us define the Reynolds number by:

$$Re = \frac{|u|D_H}{\nu} \quad (2.25)$$

in which,

- ▷ $|\mathbf{u}|$ is the depth-averaged flow velocity,
- ▷ D_H is the hydraulic diameter, defined by $D_H = 4A/P$ with A the cross sectional area of the flow and P the wetted perimeter,
- ▷ ν is the kinematic viscosity of water.

For fully developed laminar flow, i.e. $Re < 2200$, the heat transfer coefficient can be calculated by:

$$h_{wi} = \frac{NuK_w}{D_H} \quad (2.26)$$

in which,

- ▷ K_w is the thermal conductivity of water,
- ▷ Nu is the Nusselt number, which varies with the shape of the channel cross section. The Nusselt number can be defined via the keyword `NUSSELT NUMBER FOR HEAT TRANSFER BETWEEN WATER AND ICE` (default = 7.541).

For fully developed turbulent flow i.e. $Re > 2200$, the following formulas can be used:

$$\begin{aligned} h_{wi} &= C_{iw} \frac{|\mathbf{u}|^{0.8}}{D_H^{0.2}} & \text{for } T_w \leq T_f \\ h_{wi} &= C_{wi} \frac{|\mathbf{u}|^{0.8}}{D_H^{0.2}} & \text{for } T_w > T_f \end{aligned} \quad (2.27)$$

in which,

- ▷ C_{iw} and C_{wi} are two empirical constants that can be defined with the keywords: `WATER-ICE HEAT TRANSFER COEF. FOR SUPERCOOLED TURBULENT FLOW` (default = $1118.0 \text{ W.m}^{-2}.\text{K}^{-1}$) and `WATER-ICE HEAT TRANSFER COEF. FOR TURBULENT FLOW` (default = $1448.0 \text{ W.m}^{-2}.\text{K}^{-1}$) respectively.

3. Supercooling and suspended frazil ice

3.1 Suspended Frazil Ice

In nature the frazil ice crystal distribution is non-homogeneous and often follows a log-normal distribution as observed in [10] and [28]. Additionally the radius of each crystal is function of time and depends on the thermal exchanges between the particle and the surrounding water. This process, also known as the thermal growth (or decay), is a key aspect to describe the evolution frazil ice evolution in water bodies. There are two models available in KHIONE to describe frazil ice evolution, the SSC¹ model and the MSC² model, which rely on different radius discretization as shown in Figure 3.1.

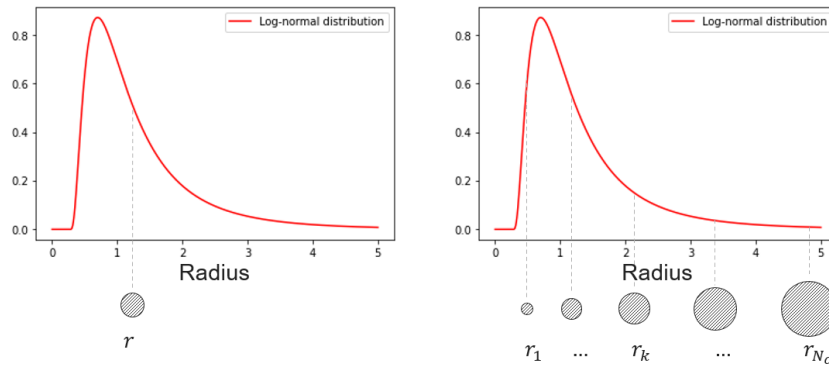


Figure 3.1: Typical log-normal distribution of frazil crystals and SSC (left) versus MSC (right) radius discretization.

In the case of the SSC model, all particles are assumed to have the same radius, noted r . Modelling thermal growth therefore consists in predicting the evolution of the global volume fraction of frazil without describing the radius changes. On the other hand, the MSC model consists in considering several classes, each one associated with a radius, noted r_k for the k^{th} class. Thermal growth (or decay) is then modelled as mass exchanges between classes which also corresponds to particles increasing (or decreasing) in size. The selection of the model depends on the number of classes selected with the keyword `NUMBER OF CLASSES FOR SUSPENDED FRAZIL`

¹SSC : single-size-class

²MSC : multiple-size-class

ICE (default = 1). If only one class is selected, the SSC model is used, otherwise the MSC model is selected. Note that the number of classes should be sufficiently large for the model to converge in radial space.

SSC model

The SSC model relies on one tracer to model frazil ice volume fraction. The radius of frazil ice crystals is assumed to be constant and representative of the whole distribution of particles in the suspension. The mass balance equation of frazil ice reads:

$$\frac{\partial C}{\partial t} + \mathbf{u} \cdot \nabla C = \frac{1}{h} \nabla \cdot (h \mathbf{v}_{t,C} \nabla C) + S_{GM} + S_{SR} + S_M, \quad (3.1)$$

in which,

- ▷ C is the frazil volume fraction,
- ▷ $\mathbf{v}_{t,C}$ is diffusivity of frazil,
- ▷ S_{GM} is the thermal growth (or melting) source term described in section 3.1.2,
- ▷ S_{SR} is the seeding rate source term described in section 3.1.5, which can be activated using the keyword `MODEL FOR FRAZIL SEEDING = 2` or `3` (default = 1).
- ▷ S_M is the mass exchange source term (deposition/erosion under the ice cover) and can be activated with the keyword `MODEL FOR MASS EXCHANGE BETWEEN FRAZIL AND ICE COVER` (default = 0).

MSC model

As opposed to the SSC model, the MSC model relies on a discrete radius distribution to describe suspended frazil ice in which a number of classes (noted N_c) are used to model the suspension. The mass balance equation of the frazil volume fraction for the k^{th} class is given by

$$\frac{\partial C_k}{\partial t} + \mathbf{u} \cdot \nabla C_k = \frac{1}{h} \nabla \cdot (h \mathbf{v}_{t,k} \nabla C_k) + S_{GM}^k + S_{SN}^k + S_{FB}^k + S_{SR}^k + S_M^k, \quad (3.2)$$

- ▷ C_k is the frazil volume fraction of the k^{th} class,
- ▷ $\mathbf{v}_{t,k}$ is diffusivity of frazil of the k^{th} class,
- ▷ S_{GM}^k is the thermal growth (or melting) source term described in section 3.1.2,
- ▷ S_{SN}^k is the secondary nucleation source term described in section 3.1.3, which can be activated using the keyword `MODEL FOR THE SECONDARY NUCLEATION` (default = 2),
- ▷ S_{FB}^k is the flocculation (and breaking) source term described in section 3.1.4, which can be activated using the keyword `MODEL FOR THE FLOCCULATION AND BREAKUP` (default = 1),
- ▷ S_{SR}^k is the seeding rate source term described in section 3.1.5, which can be activated using the keyword `MODEL FOR FRAZIL SEEDING = 2` or `3` (default = 1).
- ▷ S_M^k is the mass exchange source term by class (deposition/erosion under the ice cover) and can be activated with the keyword `MODEL FOR MASS EXCHANGE BETWEEN FRAZIL AND ICE COVER` (default = 0).

In this model, the total frazil volume fraction C is computed as

$$C = \sum_{k=1}^{N_c} C_k. \quad (3.3)$$

The number of particles per unit volume for each class is given by $n_k = C_k/V_k$ with V_k the frazil crystal volume of class k .

Note:

The flocculation and secondary nucleation source terms are only computed in the MSC model i.e. if $N_c > 1$. If $N_c = 1$ the keywords **MODEL FOR THE SECONDARY NUCLEATION** and **MODEL FOR THE FLOCCULATION AND BREAKUP** are automatically set to 0.

3.1.1 Shape of frazil crystals

Frazil crystals are supposed to have the same disc shaped geometry, as described in Figure 3.2, characterized by a radius r_k and a thickness e_k , related with a constant ratio R such that $e_k = 2r_k/R$. For the SSC description, the mean radius is defined via the keyword **FRAZIL CRYSTALS RADIUS** (default = 4.1E-4). The thickness of each crystal is defined via the ratio R which can be set with the keyword **FRAZIL CRYSTALS DIAMETER THICKNESS RATIO** (default = 10).

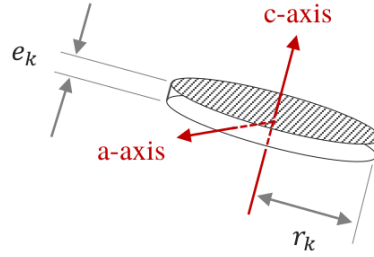


Figure 3.2: Frazil crystal shape and parameters

Note:

The number of radius provided must match the number of classes selected. For 3 classes, one could set: **FRAZIL CRYSTALS RADIUS** = 1.E-4 ; 2.E-4 ; 3.E-4

3.1.2 Thermal growth and melting

Thermal growth or melting of frazil crystals depends on the heat exchange between the particle and the surrounding water. Let us first introduce the heat flux between frazil crystals of class k and water in Equation (3.4):

$$q_k = \frac{K_w Nu_k}{l_k} (T_i - T), \quad (3.4)$$

where

- ▷ K_w is the thermal conductivity of water,
- ▷ T_i the crystal temperature assumed to be equal to the freezing temperature T_f which is either defined with the keyword **FREEZING POINT OF WATER** (default = 0) or depends on the salinity S such that $T_f(S) = -0.0575S + 0.00171S^{3/2} - 0.00021S^2$ if **SALINITY=YES**,

- ▷ l_k is the characteristic length scale of the k^{th} class. It supposed to be equal to e_k as suggested in [36],
- ▷ Nu_k is the Nusselt number associated with the k^{th} class. Different methods can be selected to estimate the Nusselt number via the keyword `MODEL FOR THE NUSSELT NUMBER` (default=1).

MSC model

The thermal growth (or decay) source term S_{GM}^k represents the net rate of volume change of class k resulting from interactions with classes $k - 1$ and $k + 1$ due to freezing or melting. Following [41] for thermal growth and [19] for the introduction of melting, the net rate of volume fraction change for the frazil class k can be defined as

$$S_{GM}^k = \frac{V_k}{\Delta V_{k-1}} [(1-H)M_k + HG_{k-1}] - \frac{V_k}{\Delta V_k} [(1-H)M_{k+1} + HG_k], \quad (3.5)$$

with

- ▷ $H = He(T_f - T)$, where He is the Heaviside function,
- ▷ V_k the volume of ice crystals,
- ▷ ΔV_k the volume ratio defined by $\Delta V_k = V_{k+1} - V_k$ which accounts for the scaling of the computed volume change to the number of particles that jump from a class to another,
- ▷ G_k and M_k are the production or depletion rates of the k^{th} class, due to thermal growth or melting of frazil crystals.

Mass exchanges between classes (or class jumps) resulting from thermal growth or decay are explained in Figure 3.3.

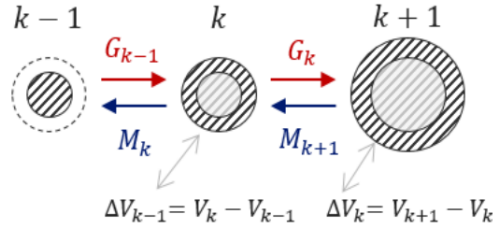


Figure 3.3: MSC model mass exchanges caused by thermal growth or melting

As explained in [12], frazil crystals are supposed to grow only from their edges because of their disc shape, which leads to the production rate for thermal growth defined by:

$$G_k = \frac{K_w Nu_k}{L_i \rho_i} (T_f - T) \frac{2}{r_k l_k} C_k, \quad (3.6)$$

whereas the melting is supposed to occur on all surfaces of the disc which leads to:

$$M_k = \frac{K_w Nu_k}{L_i \rho_i} (T_f - T) \frac{2}{l_k} \left(\frac{1}{r_k} + \frac{1}{e_k} \right) C_k, \quad (3.7)$$

where

- ▷ $\rho_i = 916.8 \text{ kg.m}^{-3}$ is the ice density,
- ▷ $L_i = 3.34 \times 10^5 \text{ J.kg}^{-1}$ the latent heat of ice fusion,
- ▷ For the first and last classes, the boundary conditions $V_0 = V_{N_c+1} = G_0 = G_{N_c} = M_{N_c+1} = 0$ are used [19].

SSC model

For the SSC frazil ice model (when only one class of frazil is selected), the source term for frazil ice is defined by:

$$S_{GM} = (1 - H)M_1 + HG_1. \quad (3.8)$$

As explained in Figure 3.4 the SSC thermal growth source term is equivalent to considering that the increase in size of a frazil crystal due to thermal growth, is instantly followed by a secondary nucleation process so that only crystals of the same radius remain. (cf. Figure 3.4). That is one of the reasons why secondary nucleation is not considered in the case of the SSC model.

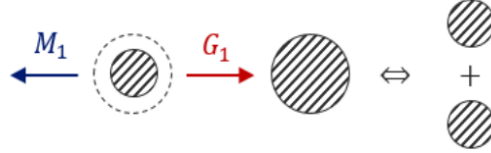


Figure 3.4: SSC model thermal growth principle

Nusslet number

The Nusselt number Nu_k model can be chosen via the keyword `MODEL FOR THE NUSSELT NUMBER` (default=1). The available models are:

- 1 : CONSTANT NUSSELT NUMBER
- 2 : WADIA (1974) & BATCHELOR (1980)

1. When `MODEL FOR THE NUSSELT NUMBER`=1, the Nusselt number is set to a constant value for each class which can be adjusted with the keyword `NUSSELT NUMBER` (default = 4).
2. When `MODEL FOR THE NUSSELT NUMBER`=2 the Nusselt number Nu_k is defined with the parametrization initially proposed in [6] and [47] and summerized in [11] and [18]. Let us define the Kolmogorov length scale noted η and defined by:

$$\eta = \left(\frac{v^3}{\varepsilon} \right)^{1/4}, \quad (3.9)$$

where

- ▷ ε is the turbulent kinetic energy dissipation rate
- ▷ v the molecular viscosity of the fluid.

For small particles, heat transfer is governed by diffusion and convection, and the Nusselt number can therefore be written as in Equation 3.10.

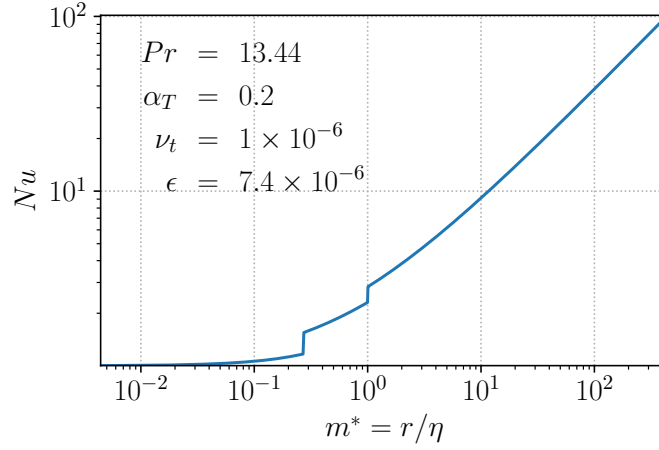
$$Nu_k = \begin{cases} 1 + 0.17m_k^*P_r^{1/2} & \text{if } m_k^* \leq P_r^{-1/2} \\ 1 + 0.55m_k^{*2/3}P_r^{1/3} & \text{if } P_r^{-1/2} < m_k^* \leq 10. \end{cases} \quad (3.10)$$

For larger particles ($m_k^* > 1$), heat transfer is governed by turbulent mixing of the boundary layer around the crystal and the Nusselt number is defined by

$$Nu_k = \begin{cases} 1.1 + 0.77\alpha_T^{0.035}m_k^{*2/3}P_r^{1/3} & \text{if } \alpha_T m_k^{*4/3} \leq 1000 \\ 1.1 + 0.77\alpha_T^{0.25}m_k^*P_r^{1/3} & \text{if } \alpha_T m_k^{*4/3} > 1000, \end{cases} \quad (3.11)$$

in which

- ▷ Pr denotes the Prandlt number, defined as the ratio between molecular and thermal diffusivity,
- ▷ α_T is the turbulent intensity defined by $\alpha_T = \frac{\sqrt{2k}}{|u|}$,
- ▷ m^* is the ratio between the radius and the Kolmogorov length scale defined by $m^* = \frac{r_k}{\eta}$.

Figure 3.5: Nusselt number as a function of the ratio m^* **Note:**

When using MODEL FOR THE NUSSELT NUMBER=2, turbulent parameters need to be estimated using MODEL FOR ESTIMATION OF TURBULENCE PARAMETERS=1 or 2. See section 3.4 for additional details.

3.1.3 Secondary nucleation

When frazil crystals collide, new nuclei are detached which increases the volume fraction of the smallest particles. This is known as the secondary nucleation process. There are two variants of secondary nucleation model implemented in KHIONE which can be selected with the keyword MODEL FOR THE SECONDARY NUCLEATION (default = 2):

```
0 : NO SECONDARY NUCLEATION
1 : SVENSSON & OMSTEDT (1994)
2 : WANG & DOERING (2005)
```

Secondary nucleation is modeled (in model 1 or 2) using an approximation of the collision frequency between particles [34]. A particle with a velocity w_k^r relative to the fluid sweeps a volume $\delta V = w_k^r \pi r_k^2 \delta t$ during δt . The collision frequency can be estimated as $f_{coll}^k \sim \tilde{n} \delta V n_k / \delta t$, in which \tilde{n} is an estimation of the average number of particles per unit volume, defined in Equation (3.12) and n_k the number of particles of class k per unit volume.

$$\tilde{n} = \max \left(\sum_{j=1}^{N_c} n_j, n_{max} \right). \quad (3.12)$$

n_{max} is a parameter used to limit collisions impact which can be tuned using the SECONDARY NUCLEATION NMAX PARAMETER (default = 6.E6). The relative velocity is estimated from the

rising and turbulent velocities such that

$$w_k^r = \sqrt{U_k^t^2 + w_k^2}, \quad (3.13)$$

with

- ▷ U_k^t the turbulent velocity of crystals estimated by $U_k^t = 2r_k \sqrt{\frac{\varepsilon}{15\nu}}$,
- ▷ w_k the buoyant rise velocity of frazil crystals. Different models can be selected via the keyword `MODEL FOR THE BUOYANCY VELOCITY` (default = 1).

Finally, volume fraction change rate due to secondary nucleation can be written as:

$$S_{SN}^k = \begin{cases} \sum_{j=2}^N \pi \tilde{n} w_j^r r_j^2 C_j & \text{if } k = 1 \\ -\pi \tilde{n} w_k^r r_k^2 C_k & \text{if } k \neq 1 \end{cases}. \quad (3.14)$$

Mass exchanges between classes due to the secondary nucleation process are schematized in Figure 3.6.

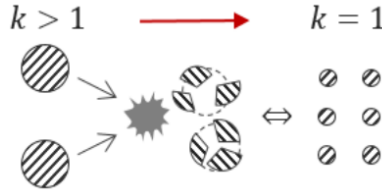


Figure 3.6: Mass exchanges between classes due to secondary nucleation

Rise velocity of frazil crystals

Different empirical approaches are proposed in the literature to estimate the rise velocity w_k . The model can be selected via the keyword `MODEL FOR THE BUOYANCY VELOCITY` (default = 2):

- 1 : DALY (1984)
- 2 : SVENSSON & OMSTEDT (1994)
- 3 : MATOUSEK (1992)
- 4 : GOSIK & OSTERKAMP (1983)
- 5 : MORSE & RICHARD (2009)

1. If `MODEL FOR THE BUOYANCY VELOCITY=1` the formulation proposed by Daly [11] for Stokes range, intermediate range and fully turbulent range is used, for which the rise velocity is given by:

$$w_k = \begin{cases} 0.08(g'r_k^2/\nu) & \text{if } r_k \leq 3 \cdot 10^{-4} \\ 0.16(g'^{0.715} \nu^{-0.428} r_k^{1.14}) & \text{if } 3 \cdot 10^{-4} < r_k \leq 1.4 \cdot 10^{-3} \\ \sqrt{g'r_k/2} & \text{if } r_k > 1.4 \cdot 10^{-3}, \end{cases} \quad (3.15)$$

in which

- ▷ $g' = \frac{2K_v g(\rho - \rho_i)}{\pi \rho}$ is the reduced gravitational acceleration,
- ▷ $K_v = 2\pi/R$ is the volumetric shape factor.

2. Svensson and Omstedt [34] simplified the previous formulation into $w_k = 32.8(2r_k)^{1.2}$ which only takes into account the intermediate range (`MODEL FOR THE BUOYANCY VELOCITY=2`).

3. If MODEL FOR THE BUOYANCY VELOCITY=3 an empirical formulation proposed by Matousek [30] is used leading to:

$$w_k = 1.31 \cdot 10^{-5} (2r_k^{0.29} e_k^{0.61} / \nu) \quad (3.16)$$

4. If MODEL FOR THE BUOYANCY VELOCITY=4 the formulation proposed by Gosik and Osterkamp in [17] for fully turbulent range is used and the rise velocity is estimated with:

$$w_k = \sqrt{\frac{4gr_k(\rho - \rho_i)}{RC_d\rho}}. \quad (3.17)$$

in which C_d is the drag coefficient.

5. If MODEL FOR THE BUOYANCY VELOCITY=5 the formulation proposed by Morse and Richard [33] is used, which reads (in mm-s units, with $d_k = 2r_k$)

$$w_k = \begin{cases} 2.025d_k^{1.621} & \text{if } d_k \leq 1.27 \text{ mm} \\ -0.103d_k^2 + 4.069d_k - 2.024 & \text{if } d_k > 1.27 \text{ mm} \end{cases} \quad (3.18)$$

A review of rise velocity formulations is plotted on Figure 3.7.

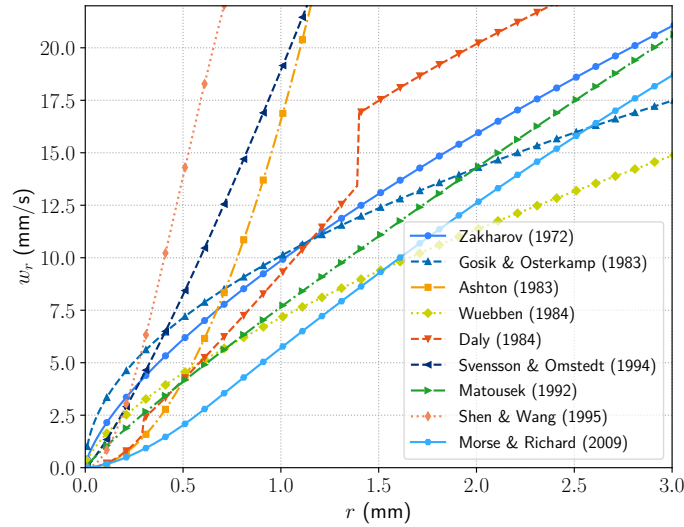


Figure 3.7: Rise velocity formulations with $R = 10$.

3.1.4 Flocculation

The flocculation model can be selected with the keyword MODEL FOR THE FLOCCULATION AND BREAKUP (default = 1):

```
0 : NO FLOCCULATION
1 : SVENSSON AND OMSTEDT (1994)
```

If MODEL FOR THE FLOCCULATION AND BREAKUP=1, the flocculation source term is defined in Equation (3.19) and schematized in Figure 3.8.

$$S_{FB}^k = \beta_{k-1}C_{k-1} - \beta_k C_k. \quad (3.19)$$

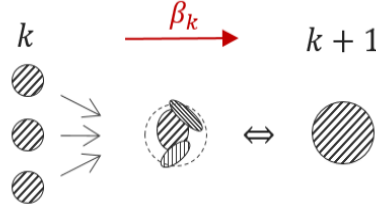


Figure 3.8: Mass exchanges between classes due to flocculation

Flocculation and breakup are supposed to result only in a net increase in scales [34]. The effectiveness of class jumps is supposed to be linearly dependent on radius:

$$\beta_k = a_{floc} \frac{r_k}{r_1}, \quad (3.20)$$

where

- ▷ a_{floc} represents the proportion of frazil crystals that move from class k to $k + 1$ per second, which can be tuned with the keyword FLOCCULATION AFLOC PARAMETER (default = 1.E3),
- ▷ r_k is the radius of the k^{th} class,
- ▷ r_1 is the radius of the first class.

3.1.5 Seeding

Modeling primary nucleation is still a major difficulty in frazil studies as the seeding process is not fully understood yet. It depends on atmospheric conditions (snow, mist) and water impurities. In KHIONE there are two ways to introduce primary nuclei in the media, which can be selected via the keyword MODEL FOR FRAZIL SEEDING (default = 1):

```
0 : NO SEEDING
1 : MINIMUM CONC. THRESHOLD
2 : CONSTANT SURFACIC SEEDING RATE
3 : BOTH OPTIONS 1 AND 2
```

1. If MODEL FOR FRAZIL SEEDING=1 a minimum threshold of frazil volume fraction is set to prevent frazil to decrease below this threshold. It is defined with a minimum number of nuclei per unit volume, which can be tuned via the keyword MINIMUM NUMBER OF FRAZIL CRYSTALS (default = 7.1586E4). If multiple classes are selected, the number of primary nuclei is equally shared between all classes. Note that the default value was obtained from optimal calibration with Carstens experiments [9] alongside a default mean radius of 4.1E-4 and a constant Nusselt number of 4.
2. If MODEL FOR FRAZIL SEEDING=2 a surfacic seeding rate is used, which corresponds to a number of crystals reaching the water column through the free surface per second, noted $\tau_{seeding}$ in $\text{crystals.m}^{-2}.\text{s}^{-1}$. The volumic seeding rate source term, which corresponds to the increase of the frazil volume fraction, noted S_{SR}^k is then defined by $S_{SR}^k = V_k \times \tau_{seeding}/h$. The surfacic seeding rate $\tau_{seeding}$ can be adjusted with the keyword FRAZIL SEEDING RATE (default = 100.). An estimation of the seeding rate based on observations has been proposed in [12] leading to a range of 3×10^{-1} to $1 \text{ crystals.cm}^{-2}.\text{s}^{-1}$.
3. Both methods of seeding can be selected by setting MODEL FOR FRAZIL SEEDING=3.

Note:

If no seeding is selected i.e. `MODEL FOR FRAZIL SEEDING=0`, the first melting event will cause a decrease of frazil volume fraction until it reaches 0 making any further thermal growth of frazil impossible due to the nature of the model. Therefore the introduction of new nuclei with seeding methods 1, 2 or 3 are mandatory to allow multiple successive freeze-up and melting sequences.

3.1.6 Deposition and erosion under the ice cover

Suspended frazil particles growing in size, may cluster together, and move up to the water surface to either form surface ice, deposit on the bottom of the ice cover, or attach on the bottom of ice pans. This upward movement is controlled by the buoyancy velocity of the frazil ice particles and the strength of turbulence mixing. The ice flocs on the water surface can also be entrained into the river flow when the turbulence intensity is strong enough to overcome their buoyancy. In the present model a sink term S_M^k is introduced in Equation 3.2 to model mass transfer between suspended frazil ice and the ice cover. Deposition and erosion can be activated with the keyword `MODEL FOR MASS EXCHANGE BETWEEN FRAZIL AND ICE COVER` (default = 0):

```
0 : NO MASS EXCHANGE
1 : DEPOSITION ONLY
2 : DEPOSITION AND EROSION
```

Frazil ice particles rise to the surface at a rate which depends on concentration and on the rise velocity defined in Equation 3.17. The sink term for each class of frazil can be expressed as

$$S_M^k = -\frac{1}{h} \int_{z_b}^{\eta} \frac{\partial w_k \bar{C}_k(z)}{\partial z} dz, \quad (3.21)$$

in which

- ▷ z_b is the bottom elevation
- ▷ η is the free surface elevation
- ▷ $\bar{C}_k(z)$ is the frazil volume fraction in the water column

To properly describe the net flux of frazil ice accumulating at the free surface, assumptions should be made on the vertical profile of frazil ice volume fraction and rise velocity but also on the physical deposition and erosion processes.

1. If `MODEL FOR MASS EXCHANGE BETWEEN FRAZIL AND ICE COVER=1` only a net deposition flux is considered. The source term S_M^k is defined such that $S_M^k = -S_{MI}^k/h$ where S_{MI}^k is defined in the section 4.5. A constant volume fraction profile and a constant buoyant rise velocity are considered leading to the following deposition/erosion source term:

$$S_M^k = -\min \left(\frac{D_k w_k C_k}{h}, \frac{C_k}{\Delta t} \right). \quad (3.22)$$

in which

- ▷ w_k is the buoyancy velocity of class k in m.s^{-1} , as defined in section 3.1.3,

- ▷ D_k is the probability of deposition of frazil particles reaching the surface for the class k (between 0 and 1), which can be set via the keyword FRAZIL UNDER COVER DEPOSITION PROBABILITY (default = 1)
- 2. If MODEL FOR MASS EXCHANGE BETWEEN FRAZIL AND ICE COVER=2 erosion and deposition are both considered. The source term S_M^k is defined such that $S_M^k = -S_{MI}^k/h$ where S_{MI}^k is defined in the section 4.5.

Note:

In addition to frazil conservation equations, a mass balance equation for the surface ice layer needs to be introduced to ensure total ice mass conservation. This can be achieved by introducing a dynamic ice cover model with the keyword DYNAMIC ICE COVER = YES (default=NO) as described in section 4.2.

3.2 Thermal balance

The water fraction of the water-ice mixture is characterized by a temperature, subject to a heat balance defined as:

$$\frac{\partial}{\partial t} [(1-C)T] + \nabla \cdot [(1-C)\mathbf{u}T] = \frac{1}{h} \nabla \cdot (h\mathbf{v}_{t,T} \nabla [(1-C)T]) + \frac{\phi_s}{h\rho c_p} - \frac{1}{\rho c_p} (S_L + S_L^{ic}) \quad (3.23)$$

where

- ▷ $c_p = 4.1855 \times 10^3 \text{ J.kg}^{-1}.\text{K}^{-1}$ is the specific heat of water,
- ▷ ϕ_s is the net heat flux at the free surface in W.m^{-2} ,
- ▷ S_L is the heat source due to melting or freezing of frazil ice expressed in W.m^{-3} ,
- ▷ S_L^{ic} is the heat source due to melting or freezing of the ice cover in W.m^{-3} , defined in section 4.4.

The net heat flux at free surface ϕ_s is equal to ϕ_{aw} in absence of ice cover. If ice cover is present, the net heat flux received by water is combination of the fraction of the heat flux coming from the atmosphere to the water surface and the heat exchange with the ice cover layer, therefore ϕ_s can be expressed as:

$$\phi_s = (1 - C_i)\phi_{aw} + C_i(\phi_{iw} + \phi_{ai}), \quad (3.24)$$

in which

- ▷ C_i is the surface ice fraction (portion of free surface covered by ice),
- ▷ ϕ_{iw} is the convective heat flux between the surface ice layer and the water column.

The heat source due to melting or freezing can be expressed as:

$$S_L = \rho L_i \delta_w - \rho c_p T_i \delta_w, \quad (3.25)$$

where

- ▷ T_i the crystal temperature, assumed to be equal to the freezing temperature,
- ▷ δ_w is the water volume change rate (s^{-1}) due to frazil ice evolution, expressed as

$$\delta_w = -\frac{\rho_i}{\rho} \sum_{k=1}^{N_c} S_{GM}^k. \quad (3.26)$$

For simplicity's sake, let us neglect S_L^{ic} , Equation (3.23) can be developed as:

$$(1-C) \frac{\partial T}{\partial t} + (1-C) \mathbf{u} \cdot \nabla T = \frac{1}{h} (1-C) \nabla \cdot (h \mathbf{v}_{t,T} \nabla T) - 2 \mathbf{v}_{t,T} \nabla T \cdot \nabla C + \frac{\phi_s}{h \rho c_p} - \delta_w \left(T - T_f + \frac{L_i}{c_p} \right). \quad (3.27)$$

Additionally, the term $2 \mathbf{v}_{t,T} \nabla T \cdot \nabla C$ in Equation (3.27) can be neglected after [19], considering the hypothesis that $C \ll 1$. Hence, the heat balance Equation (3.28) is obtained.

$$\frac{\partial T}{\partial t} + \mathbf{u} \cdot \nabla T = \frac{1}{h} \nabla \cdot (h \mathbf{v}_{t,T} \nabla T) + \frac{\phi_s}{h \rho c_p (1-C)} + \frac{\rho_i}{\rho (1-C)} \left(T - T_f + \frac{L_i}{c_p} \right) \sum_{k=1}^{N_c} S_{GM}^k. \quad (3.28)$$

Equation (3.28) can be further simplified by considering $C \ll 1$ and $T - T_f \ll \frac{L_i}{c_p}$, which leads to:

$$\frac{\partial T}{\partial t} + \mathbf{u} \cdot \nabla T = \frac{1}{h} \nabla \cdot (h \mathbf{v}_{t,T} \nabla T) + \frac{\phi_s}{h \rho c_p} + \frac{\rho_i L_i}{\rho c_p} \sum_{k=1}^{N_c} S_{GM}^k. \quad (3.29)$$

Both Equations (3.28) and (3.29) are implemented in KHIONE and can be selected via the keyword ENERGY BALANCE VERSION (default = 1):

```
1 : SIMPLIFIED ENERGY BALANCE
2 : FULL ENERGY BALANCE
```

For the SSC frazil ice model (when only one class of frazil is selected), Equations (3.28) and (3.29) still hold by replacing $\sum_{k=1}^{N_c} S_{GM}^k$ by S_{GM} . Note that S_L^{ic} is taken into account in both formulations in presence of an ice cover.

3.3 Salinity balance

The salinity can be activated in the model with the keyword SALINITY (default = NO). If SALINITY=YES, the salinity balance is given by:

$$\frac{\partial S}{\partial t} + \mathbf{u} \cdot \nabla S = \frac{1}{h} \nabla \cdot (h \mathbf{v}_{t,S} \nabla S) + S_R, \quad (3.30)$$

in which

- ▷ $\mathbf{v}_{t,S}$ is the turbulent diffusivity,
- ▷ S_R is the salt rejection source term caused by the freezing or melting of frazil ice.

Salt rejection can be expressed as a function of the water phase rate of volume change δ_w . The salinity rejection source can be calculated as in Equation (3.31)

$$S_R = \frac{\rho_i}{\rho} (S - S_i) \sum_{k=1}^{N_c} S_{GM}^k, \quad (3.31)$$

with

- ▷ S_i the salinity of frazil crystals assumed to be equal to zero.

For the SSC frazil ice model (when only one class of frazil is selected), Equation (3.31) still holds by replacing $\sum_{k=1}^{N_c} S_{GM}^k$ by S_{GM} .

3.4 Turbulence

Turbulence parameters required to compute the different sources defined above can be estimated via different approaches selected via the keyword `MODEL FOR ESTIMATION OF TURBULENCE PARAMETERS` (default = 1):

```
0 : CONSTANT VALUES
1 : MIXING LENGTH MODEL, SHEN (2010)
2 : K-EPS MODEL OF TELEMAC-2D
```

1. If `MODEL FOR ESTIMATION OF TURBULENCE PARAMETERS=0`, the turbulent kinetic energy k , the turbulent kinetic energy dissipation rate ε and the turbulent intensity α_T need to be provided with the keyword `CONSTANT TURBULENCE PARAMETERS` (default: 9.6×10^{-4} ; 12×10^{-4} ; 8.7×10^{-2}). These constant parameters will only affect the computation of the Nusselt number (cf. section 3.1.2).
2. If `MODEL FOR ESTIMATION OF TURBULENCE PARAMETERS=1`, the model suggested in [41] is used which relies on a depth averaged integration of k and ε profiles defined as in Equations (3.32) and (3.33).

$$k(z) = \frac{u_*^2}{\sqrt{C_\mu}} \left(1 - \frac{z}{h}\right), \quad (3.32)$$

$$\varepsilon(z) = \frac{u_*^3}{\kappa z} \left(1 - \frac{z}{h}\right), \quad (3.33)$$

in which u_* is the friction velocity. The profiles are integrated between the upper bound of the viscous boundary layer and the free surface [41].

3. If `MODEL FOR ESTIMATION OF TURBULENCE PARAMETERS=2` turbulence parameters are estimated using the k - ε solver from `TELEMAC-2D`.

Turbulent viscosities are then computed as $\nu_t = C_\mu \frac{k^2}{\varepsilon}$.

3.5 Clogging or frazil accretion on racks

Frazil accretion on racks can occur when the water temperature is supercooled. While there is no analytical formulation available, a few laboratory and field studies have been published on the topic ([14], [3], [4] and [37]).

The growth of ice on the rack is predominately due to the deposition of suspended frazil on the rack bars ([13]). The Figure 3.9 shows the typical processes of frazil accretion on the trash rack bars ([14]).

`KHIONE` allows the accretion of ice on either one set of bars (vertical or horizontal) or a combined mesh (vertical and horizontal), the difference being based on the geometry of frazil accretion and blockage. It is important to note that the retro-action of the accumulated ice on the flow is not taken into account.

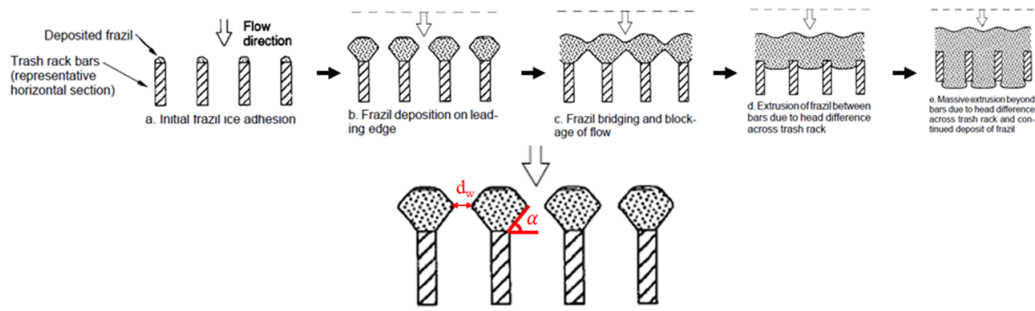


Figure 3.9: Stages of frazil accretion on a rack of vertical bars

3.5.1 Inputs and outputs

This physical process can be activated with the keyword `CLOGGING ON BARS = YES` (default is NO).

It is possible to activate this process on a liquid boundary, by specifying its number with the keyword `CLOGGED BOUNDARY NUMBERS` (default = 0). If several boundary numbers are given, the clogging process appends on all of them.

It is also possible to simulate the clogging on sections in the middle of the computational domain. The keyword `CLOGGED SECTIONS` must then be given, with the nodes corresponding to the section extremity. For example, if one wants to compute the clogging on two sections, the first between nodes 125 and 256 and the second between nodes 267 and 52, the steering file should contain the keyword `CLOGGED SECTIONS = 125;256 ; 267;52`.

The results of the clogging are saved in the file with the name specified with the keyword `CLOGGING RESULTS FILE`. It contains the accumulated mass and volume of ice on the rack and the available area for the water in an ASCII file for all the clogged sections and boundaries.

3.5.2 Clogging on a set of vertical or horizontal bars

The physical properties of the bars are set through the keyword `PHYSICAL CHARACTERISTICS OF THE INTAKE RACK`. The dimension of this keyword is 4. The default value is 0.06; 0.01; 0.06; 0.01. The values represent:

1. distance between the centre of the transverse bars,
2. diameter of the transverse bars,
3. distance between the centre of the vertical bars,
4. diameter of the vertical bars.

To consider only vertical bars, the diameter of horizontal bars must be set to zero and vice versa. In the following, the diameter of the bars set with this keyword corresponds to the variable l_B , and the distance between the bars is used to compute n_B the number of bars in the section.

It is estimated from Figure 3.9 that the angle α between the edge of frazil accumulation and the transverse direction is 55° . The width of the gap between two bars with ice accumulation is d_w . Since the flow passes through the submerged rack, it is assumed that the frazil ice is uniformly

distributed over its cross-section. This assumption could be removed at a later stage.

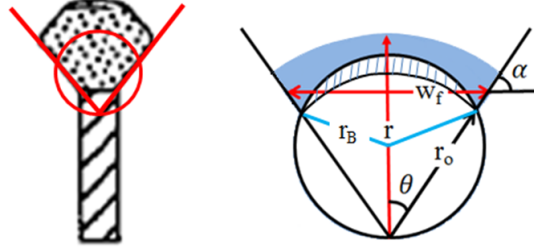


Figure 3.10: Geometry of frazil accretion on a bar

The frazil deposition is assumed to start from the front face of the bars, as shown in the blue colored arch within the angle 2θ in Figure 3.10 above, where θ is about $35^\circ = 90^\circ - 55^\circ$ by default. The keyword `ANGLE OF ACCUMULATED ICE` (default = 35) allows to modify the value of θ . The deposition efficiency of the frazil is assumed to be 1.0 to be conservative.

The volume of frazil ice accumulation on a bar can be expressed as

$$\nabla = [\theta r^2 - (r_0^2 \sin \theta \cos \theta + 2\theta r_B^2 - r_B^2 \sin 2\theta \cos 2\theta)] l_B \quad (3.34)$$

in which,

- ▷ ∇ is the volume of frazil ice accumulation,
- ▷ r is the radius of the frazil ice accumulation,
- ▷ r_0 is the initial radius before the frazil ice accumulation, and
- ▷ l_B is the length of the bar.

The volumetric rate of frazil ice accumulation can be written as

$$\frac{d\nabla}{dt} = 2\theta r l_B \frac{dr}{dt} \quad (3.35)$$

or

$$\frac{d\nabla}{dt} = \frac{q_{cv} w_f \alpha_f}{1 - e_f} \quad (3.36)$$

in which,

- ▷ $q_{cv} = V_f H C_v$ is the unit width discharge of frazil ice volume,
- ▷ V_f is the frazil velocity, assumed to be equal to water velocity normal to the grid,
- ▷ C_v is volumetric frazil ice concentration,
- ▷ $w_f = 2r \sin \theta$ is the frontal width for the frazil ice accumulation,
- ▷ α_f is the deposition coefficient, 1.0, and

- ▷ e_f is the porosity, set to 0.67 by default after [4]. This value can be modified through the keyword `POROSITY OF ACCUMULATED ICE`.

Equations (3.35) and (3.36) give

$$\frac{dr}{dt} = \frac{q_{cv}}{\theta l_B (1 - e_f)} \sin \theta \alpha_f \quad (3.37)$$

and

$$\frac{dw_f}{dt} = \frac{q_{cv}}{\theta l_B (1 - e_f)} 2 \sin^2 \theta \alpha_f \quad (3.38)$$

Equation (3.38) determines the growth rate of the frontal width of the frazil ice accumulation. Its finite difference form is

$$w_f^{i+1} = w_f^i + \Delta t \frac{q_{cv}}{\theta l_B (1 - e_f)} 2 \sin^2 \theta \alpha_f \quad (3.39)$$

The flow passage through the openings between two bars can be calculated:

$$d_w = d - w_f \quad (3.40)$$

in which,

- ▷ d is centre to centre distance between two bars, and
- ▷ d_w is the width of the available flow passage.

3.5.3 Clogging on a grid of vertical and horizontal bars

The calculations of the frazil clogging on the vertical and transverse bars follow the same procedures. Therefore, the available flow area for one grid can be calculated as

$$A_w = D_{w,V} l_{B,V} (n_V - 1) - w_{f,T} [l_{B,T} - n_V \max(d_{B,V}, w_{f,T})] n_T \quad (3.41)$$

in which,

- ▷ subscripts V and T represent the vertical and transverse bars,
- ▷ n_B is number of bars, and
- ▷ l_B is the length of the bar

4. Ice cover

4.1 Introduction on ice cover processes

Ice accumulating on the surface of a water body can take many forms from slush ice in its early stage of formation to rigid ice floes. Eventually it can significantly grow to form a thick solid ice cover. Initially, the ice cover can result from the buoyancy of frazil floes reaching and accumulating at free surface or result from a direct growth from river banks also known as border ice growth. This wide zoology of ice types and processes offers a large variety of approaches when it comes to model the ice cover formation and dynamics. The ice cover can be characterized by the several physical variables which are:

- ▷ the thickness, noted t_i ,
- ▷ the surface fraction, noted C_i , describing the horizontal distribution of ice cover,
- ▷ the horizontal velocity $\mathbf{u}_i = [u_i, v_i]^T$, describing the ice cover dynamics.

To model an ice cover, one might want to predict its formation (evolution of C_i), its evolution in thickness (evolution of t_i) but also its motion (\mathbf{u}_i). One might also want to assess its impact on hydrodynamics to properly model the hydrodynamic flows underneath the ice layer as well as all other interactions the ice cover has with other tracers such as temperature (heat exchanges between ice cover and water, see section 2.3.6) and suspended frazil ice (mass exchanges between ice cover and suspended frazil ice, see section 3.1.6).

In KHIONE two main types of ice cover are considered depending on whether it moves or is static. The models that are used to describe t_i , C_i and \mathbf{u}_i are either conservation equations in the dynamic case or a mix of empirical relations and deterministic equations in the static case. The models are described in the following sections:

- ▷ Dynamic ice cover (see section 4.2)
- ▷ Static ice cover (see section 4.3)

Note that both type of ice cover can be activated in a simulation at the same time, in which case the different types of ice are considered to form distinct layers. The total ice thickness is then computed as the sum of all ice layers' thicknesses and the total surface fraction is considered as the max of all layers' surface fraction in first approximation.

4.2 Dynamic ice cover

A simple dynamic ice cover model can be activated with the keyword `DYNAMIC ICE COVER = YES` (default = NO). The model consist in making the assumption that the ice cover is convected with the same velocity as the water column. This model rely on two conservation equations to describe the ice cover. One on the surface ice fraction and the second on the ice thickness. This model is best suited for the early stage of ice cover formation when it is mainly formed by slush ice or grease ice. The governing equations for ice cover surface fraction and ice cover thickness read:

$$\frac{\partial C_i}{\partial t} + \mathbf{u}_i \cdot \nabla C_i = \frac{1}{h} \nabla \cdot (h \mathbf{v}_i \nabla C_i) + S_M^c + S_\phi^c, \quad (4.1)$$

and

$$\frac{\partial t_i}{\partial t} + \mathbf{u}_i \cdot \nabla t_i = \frac{1}{h} \nabla \cdot (h \mathbf{v}_i \nabla t_i) + S_M^t + S_\phi^t, \quad (4.2)$$

in which

- ▷ \mathbf{u}_i (m/s) is the velocity of the ice layer, supposed to be equal to the water velocity \mathbf{u} ,
- ▷ C_i (-) is the surface fraction of ice at the surface,
- ▷ t_i (m) is the ice cover thickness,
- ▷ \mathbf{v}_i is the ice cover diffusivity,
- ▷ S_M^c and S_M^t are the ice cover fraction and thickness mass exchange sources respectively (which come from erosion and deposition), defined as functions of the mass exchange sources S_{MI}^k which are defined in section 4.5,
- ▷ S_ϕ^c and S_ϕ^t are the ice cover fraction and thickness thermal expansion sources respectively, defined as functions of the thermal expansion source S_ϕ defined in section 4.4.

The total volume of ice per surface area can therefore be computed as $C_i \times t_i$ (m³/m²). To compute the sources S_M^c and S_M^t from S_{MI}^k , as well as the sources S_ϕ^c and S_ϕ^t from S_ϕ , two phases are considered is the ice cover evolution process:

- ▷ first, the ice cover thickness is supposed to be constant and equal to t_{imin} (m) which can be set with the keyword `MINIMAL THICKNESS OF ICE COVER` (default = 0.001). The ice cover sources are therefore supposed to only increase the surface fraction of ice C_i until it reaches its maximum value of 1.
- ▷ Once $C_i = 1$, slush ice can no longer accumulate horizontally, and therefore starts to accumulate underneath the ice layer, increasing the ice cover thickness.

Finally, the deposition/erosion source term S_M^c reads:

$$S_M^c = \begin{cases} (\sum_{k=1}^{N_c} S_{MI}^k) / (1 - \alpha_t) t_{imin} & \text{if } C_i < 1 \\ 0 & \text{else} \end{cases}, \quad (4.3)$$

in which,

- ▷ t_{imin} (m) is the minimal ice cover thickness which can be set with the keyword `MINIMAL THICKNESS OF ICE COVER` (default = 0.001).
- ▷ this source term is consistent with the definition of S_M^k , as defined in section 3.1.6, to ensure the mass conservation of ice.

- ▷ α_t is the porosity of surface ice which can be set with the keyword `POROSITY OF SURFACE ICE` (default = 0.4).

The deposition/erosion source term S_M^t reads:

$$S_M^t = \begin{cases} (\sum_{k=1}^{N_c} S_{MI}^k)/(1 - \alpha_t) & \text{if } C_i \geq 1 \\ 0 & \text{else} \end{cases} \quad (4.4)$$

The sources S_ϕ^c and S_ϕ^t are defined similarly, adding the assumption that S_ϕ^c is only taken into account if melting i.e. if $S_\phi < 0$. Finally, flux limiters are introduced to prevent the source terms from leading to $C_i > 1$, $C_i < 0$ or $t_i < t_{imin}$.

4.3 Static ice cover (border ice)

As its name suggests, border ice is a type of ice that grows from the banks of a river, coastline or lake. This type of ice is always supposed to be stucked to the border of the computational domain, such that ice velocity is neglected i.e. $\mathbf{u}_i = 0$. This process can be activated with the keyword `BORDER ICE COVER = YES` (default = NO). Ice cover usually first appears as static border ice along banks. Static border ice growth is computed by proximity to border edges of the finite element mesh (either mesh boundaries or by accumulation of border ice where border ice has formed already).

If the thermal and mechanical conditions for static border ice growth are met on a node adjacent to the border ice boundary, ice growth will proceed from the boundary toward that node. The growth continues from node to node until the conditions exceed the thresholds for static border ice growth. [29] proposed the following thresholds for static border ice formation:

1. the water surface temperature, T_{ws} (°C), is less than a critical value, T_{cr} (°C), for static border ice formation. The critical temperature is -1.1°C by default based on data from River Ohre but can be modified through the keyword `CRITICAL WATER TEMPERATURE FOR STATIC BORDER ICE`,
2. the buoyant velocity of frazil, v_b (m/s), is greater than the vertical turbulence velocity, v_z' (m/s),
3. the local depth-averaged velocity, \mathbf{u} (m/s), is less than the critical velocity for static border ice formation, V_{cr} (m/s). V_{cr} can be set with the keyword `CRITICAL VELOCITY FOR STATIC BORDER ICE` (default = 0.07).

The first condition is a thermal consideration and the second and third are hydrodynamic considerations. It is noted that the presence of frazil ice is not used as a threshold.

The water surface temperature is computed from the depth-averaged water temperature using an empirical relationship [29] [31].

$$T_{ws} = T_w - \frac{\phi_{wa}}{1130|\mathbf{u}| + bW} \quad (4.5)$$

in which,

- ▷ T_w is the depth-averaged water temperature (°C),

- ▷ ϕ_{wa} is the rate of net heat loss from the water to the atmosphere (W/m^2) calculated in (2.2),
- ▷ W is the wind velocity (m/s), and
- ▷ b is the wind coefficient related to channel surface width B in the wind direction:

$$\begin{cases} b = B & \text{if } b \leq B \\ b = -0.9 + 5.87 \log B & \text{if } b > B \end{cases} \quad (4.6)$$

The value of B (m) is given with the keyword CHANNEL WIDTH FOR THE COMPUTATION OF SURFACE TEMPERATURE (default = 15).

The buoyancy velocity of the frazil particles was given by [29]:

$$v_b = -0.025T_{ws} + 0.005 \quad (4.7)$$

The expression for the vertical turbulence velocity, including the effect of wind-generated turbulence was developed by [25]:

$$v'_z = \left[\left(C_T^{0.5} g^{0.5} \frac{un_b}{h^{\frac{1}{6}}} \right)^3 + C_{w*} \left(C_D \frac{\rho_a}{\rho} \right)^{\frac{3}{2}} W^3 \right]^{1/3} \quad (4.8)$$

in which,

- ▷ C_T is a coefficient which relates bed shear stress to turbulent fluctuation velocity, which was found to lie between 0.2 and 0.3 [39] and fixed to 0.25,
- ▷ n_b is the bed Manning's coefficient,
- ▷ h is the water depth (m),
- ▷ C_{w*} is a constant explaining the efficiency of wind energy utilization, which was selected based on experimental observations, assumed to be 1.0, and
- ▷ C_D is the wind drag coefficient equal to 1.3×10^{-3} .

Based on past ice modelling studies (for instance the freeze up of the upper St. Lawrence River, Canada), the critical water surface temperature and depth-averaged water velocity were calibrated:

- The critical water surface temperature given by [29] $T_{cr} = -1.1$ °C was found to work well.
- [32] found that when $V/V_c < 0.167$, static border ice or skim ice will grow. V_c is the maximum depth-averaged velocity for border ice formation, i.e. when $V > V_c$ no border ice will grow.
Later, [42] found $V_c = 1.2$ ft/s. Based on this, the critical velocity for static border ice formation is set by default at $V_{cr} = 0.07$ m/s.

Once the conditions are met for the formation of border ice, the surface concentration of the border ice cover is set to $C_i = 1$. Additionally, the evolution of the ice cover thickness is governed by the following equation:

$$\frac{\partial t_i}{\partial t} = S_\phi + \sum_{k=1}^{N_c} S_{MI}^k, \quad (4.9)$$

in which

- ▷ t_i (m) is the ice cover thickness,
- ▷ v_i is the ice cover diffusivity,
- ▷ S_ϕ is the ice cover thermal expansion source term defined in section 4.4.
- ▷ S_{MI}^k are the mass exchanges with suspended frazil ice defined in section 4.5

4.4 Thermal growth and decay of ice floes and ice cover

The thickness of an ice floe or an ice cover changes due to thermal growth and decay as a result of heat exchange with the atmosphere and the river water. The rate of ice thickness growth or decay is governed by heat exchanges at the top and bottom surfaces, and heat conduction in the ice cover [46]. The effect of water accumulation over melting ice on the dissipation rate is insignificant [1]. Ice cover thickness can affect the flow cross-sectional area, and hence velocity of flow. Ice cover thickness is also an important parameter in determining the stability of an ice cover and its breakup. The formulation for both ice floe and ice cover thickness growth and decay are essentially the same. Ice floes can be viewed as a moving ice cover from the point of view of thermal growth and decay.

The equation governing the temperature distribution over the thickness of an ice cover is

$$\rho_i c_i \frac{\partial T}{\partial t} = - \frac{\partial}{\partial z} \left(k_i \frac{\partial T}{\partial z} \right) + \phi_v(z, t) \quad (4.10)$$

in which

- ▷ z is the vertical distance measured downward from the top surface,
- ▷ T is the temperature in the cover,
- ▷ k_i is the thermal conductivity of ice,
- ▷ ϕ_v is the rate of internal heating of the cover due to absorption of penetrated short wave radiation.

For a solid ice cover of thickness t_i , boundary conditions at the top and bottom surfaces of the cover are

$$\begin{aligned} \rho_i L_i \frac{dt_i}{dt} &= -\phi_{ai} - k_i \frac{\partial T}{\partial z} & \text{at } z = 0 \\ \rho_i L_i \frac{dt_i}{dt} &= -\phi_{wi} + k_i \frac{\partial T}{\partial z} & \text{at } z = t_i \end{aligned} \quad (4.11)$$

At steady state, (4.10) gives a linear temperature distribution if the internal heating $\phi_v(z, t)$ is neglected. This quasi-steady state assumption has been shown to be acceptable for river ice covers because of the relatively small thickness [15].

Time dependent ice thickness growth and decay can be determined by assuming one-dimensional quasi-steady state calculations at each time step. The thickness of the ice cover is supposed to be small compared to the horizontal dimensions of the ice sheet so that the heat exchanges at the boundaries can be neglected. The ice sheet is also supposed to grow from the bottom where its temperature is equal to T_f at steady state. The rate of change of ice cover thickness can be calculated by

$$\rho_i L_i S_\phi = -\frac{\hat{\phi} + \beta(T_a - T_f)}{\beta r_{th}} - \phi_{wi} \quad (4.12)$$

in which,

- ▷ β is the heat exchange coefficient at the surface of the ice cover,
- ▷ $\hat{\phi}$ is the total heat flux from atmosphere to the the free surface minus the convective flux i.e. $\hat{\phi} = \phi_{ai} - \beta(T_a - T_s)$, in which T_s is the surface temperature of the ice cover,
- ▷ ϕ_{wi} is the heat flux between water and the ice cover,
- ▷ r_{th} is the equivalent thermal resistance of the ice cover and the convective boundary layer at the surface.

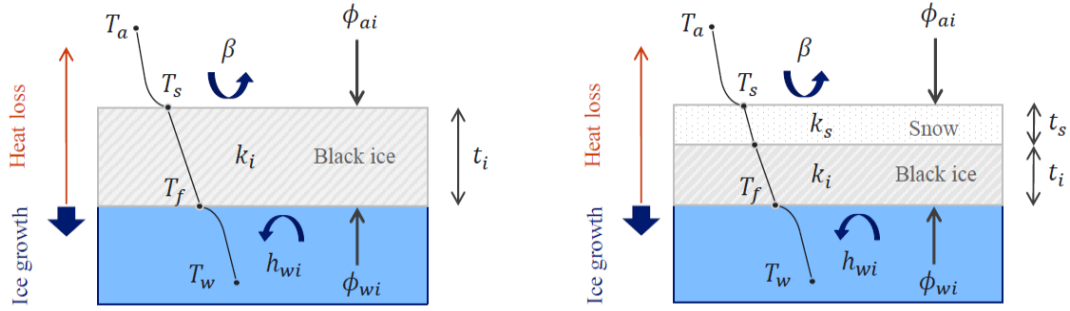


Figure 4.1: Thermal growth of the ice cover illustration

The thermal resistance depends on the vertical layering of the different types of ice composing the ice cover. If the ice cover is only composed of black ice, the thermal resistance is given by:

$$r_{th} = \frac{t_i}{k_i} + \frac{1}{\beta} \quad (4.13)$$

in which,

- ▷ k_i is the thermal conductivity of black ice.

In some meteorological conditions, snow can accumulate on top of the ice cover, which therefore impacts the thermal resistance of the ice cover, which is given by:

$$r_{th} = \frac{t_i}{k_i} + \frac{t_s}{k_s} + \frac{1}{\beta} \quad (4.14)$$

in which,

- ▷ k_s is the thermal conductivity of snow.
- ▷ t_s is the thickness of the snow layer on top of the ice cover.

The thermal growth or decay of the ice cover impacts water temperature under the ice cover, so that $S_L^{ic} = -\rho_i L_i C_i S_\phi / h$.

Note:

- ▷ The accumulation of snow is not yet taken into account in KHIONE and the ice cover is supposed to be only composed of black ice.
- ▷ The surface temperature of the ice cover T_s being unknown, the convective heat flux $\beta(T_a - T_s)$ is never computed.

4.5 Mass exchange between suspended frazil ice and ice cover

The frazil deposition/erosion source term can be activated with the keyword MODEL FOR MASS EXCHANGE BETWEEN FRAZIL AND ICE COVER (default = 0).

```
0 : NO MASS EXCHANGE
1 : DEPOSITION ONLY
2 : DEPOSITION AND EROSION
```

1. If MODEL FOR MASS EXCHANGE BETWEEN FRAZIL AND ICE COVER=1 only a net deposition flux is considered. The total volume of ice in m^3 that accumulate at the free surface, on an elementary area ΔS during a time step Δt noted ΔV_i , is expressed as a function of the buoyancy velocity and suspended frazil ice volume fractions, such that:

$$\Delta V_i = \sum_{k=1}^{N_c} D_k w_k C_k \Delta t \Delta S \quad (4.15)$$

in which,

- ▷ N_c is the number of frazil class,
- ▷ C_k is the frazil volume fraction of class k ,
- ▷ w_k is the buoyancy velocity of class k in $m.s^{-1}$, as defined in section 3.1.3,
- ▷ D_k is the probability of deposition of frazil particles reaching the surface for the class k (between 0 and 1), which can be set via the keyword FRAZIL UNDER COVER DEPOSITION PROBABILITY (default = 1).

Noting $\Delta V_i = \Delta(C_i t_i) \Delta S$, the evolution of the ice cover due to deposition/erosion can therefore be expressed as:

$$\frac{\partial C_i t_i}{\partial t} = \sum_{k=1}^{N_c} S_{MI}^k \quad (4.16)$$

in which,

- ▷ C_i is the ice cover surface fraction,
- ▷ t_i is the ice cover thickness,
- ▷ S_{MI}^k is the ice cover deposition/erosion source term defined as

$$S_{MI}^k = \min \left(D_k w_k C_k, \frac{C_k h}{\Delta t} \right) \quad (4.17)$$

The threshold in the definition of S_{MI}^k is designed such that the amount of frazil accumulating under the ice cover cannot be greater than the total suspended frazil volume in the water column at that time. Note that the frazil deposition/erosion source term S_M^k is derived from S_{MI}^k such that $S_M^k = -S_{MI}^k/h$ (see section 3.1.6).

2. If MODEL FOR MASS EXCHANGE BETWEEN FRAZIL AND ICE COVER=2 erosion and deposition are both considered. The total volume of ice in m^3 that accumulate at the free surface, on an elementary area ΔS during a time step Δt noted ΔV_i , can be expressed as:

$$\Delta V_i = \sum_{k=1}^{N_c} (D_k w_k C_k - E_k C_i t_i (1 - \alpha_t)) \Delta t \Delta S \quad (4.18)$$

in which,

- ▷ N_c is the number of frazil class,
- ▷ C_k is the frazil concentration of class k ,
- ▷ w_k is the buoyancy velocity of class k , as defined in section 3.1.3,
- ▷ D_k is the probability of deposition of frazil particles reaching the surface for the class k (between 0 and 1), which can be set via the keyword FRAZIL UNDER COVER DEPOSITION PROBABILITY (default = 1),
- ▷ E_k is the coefficient of re-entrainment rate of surface ice per unit area in s^{-1} for the class k , which can be set via the keyword FRAZIL UNDER COVER REENTRAINMENT COEFFICIENT (default = 1.E-4),
- ▷ α_t is the porosity of surface ice which can be set with the keyword POROSITY OF SURFACE ICE (default = 0.4).

The source term S_{MI}^k is then defined as previously explained.

4.6 Ice cover impact on hydrodynamics

The presence of an ice cover leads to an increase in the surface pressure due to the weight of the ice cover. As for the atmospheric pressure, the gradient of ice cover thickness produces a moment source term that needs to be taken into account. Additionally, the water column is affected by an under cover friction which also requires proper modeling. In this section, these two effects of ice cover on the hydrodynamics are addressed. These processes can be activated in KHIONE with the keyword ICE COVER IMPACT ON HYDRODYNAMIC = YES (default = NO).

4.6.1 Friction source term

Two under cover friction models can be chosen, using the keyword MODEL FOR UNDER COVER FRICTION (default = 2), with the following choices:

- 1 : FRICTION ON THE ENTIRE WATER COLUMN
- 2 : FRICTION COMPUTED WITH RATIO

1. When MODEL FOR UNDER COVER FRICTION=1 the under cover friction is solved in a similar fashion as for the bottom friction considering the whole water column has an effect on both bottom and ice cover friction terms. The friction coefficient of the ice cover n_i can be set with the keyword ICE FRICTION COEFFICIENT (default = 0.04) and is associated to the friction law set with the keyword LAW OF ICE COVER FRICTION. This is an interger between 0 and 5 to compute the following friction source terms:

▷ 0: no friction,

▷ 1: Haaland friction law writes $S_{fi} = \frac{\mathbf{u}|\mathbf{u}|}{8h \left(-0.6 \log_{10} \left(\left(\frac{6.9 \cdot 10^{-6}}{4hu} \right)^3 + \left(\frac{n_i}{14.8h} \right)^{3.33} \right) \right)^2}$,

▷ 2: Chézy friction law writes $S_{fi} = \frac{g\mathbf{u}|\mathbf{u}|}{n_i^2 h}$,

▷ 3: Strickler friction law writes $S_{fi} = \frac{g\mathbf{u}|\mathbf{u}|}{n_i^2 h^{4/3}}$,

▷ 4: Manning friction law writes $S_{fi} = \frac{n_i^2 g\mathbf{u}|\mathbf{u}|}{h^{4/3}}$,

▷ 5: Nikuradse friction law writes $S_{fi} = \frac{k^2 \mathbf{u}|\mathbf{u}|}{h \log^2 \left(\frac{11.036h}{n_i} \right)}$.

in which:

▷ \mathbf{u} is the water depth averaged velocity (m/s),

▷ h is the water depth (m),

▷ g is the gravity constant (m/s²),

▷ k is the von Karman constant (-).

The total friction force is then computed as:

$$S_f = S_{fi} + S_{fb}. \quad (4.19)$$

2. When MODEL FOR UNDER COVER FRICTION=2 the under cover friction as well as the bottom friction are computed with ratios corresponding to the fraction of water depth that is affected by the ice or the bottom respectively. For a static ice cover, or for an ice cover with a velocity $\mathbf{u}_i = 0$, the ratio of the depth affected by the bottom friction α_b reads:

$$\alpha_b = \frac{1}{1 + \left(\frac{n_i^2}{n_b^2} \right)^{3/4}}, \quad (4.20)$$

with n_i the under cover Manning's coefficient and n_b the bottom Manning's coefficient, and the ratio affected by the under cover friction α_i is then deduced with the relation:

$$\alpha_i = (1 - \alpha_b). \quad (4.21)$$

The Manning law then becomes:

$$S_{fk} = \frac{n_k^2 g \mathbf{u}|\mathbf{u}|}{(\alpha_k h)^{4/3}}, \quad (4.22)$$

where $k = i$ for under cover friction and $k = b$ for bottom friction. The total friction force is then computed as:

$$S_f = S_{fi} + S_{fb}. \quad (4.23)$$

Note:

If MODEL FOR UNDER COVER FRICTION = 2:

- ▷ Only Manning and Strickler laws are available for under cover friction and bottom friction.
- ▷ In presence of ice cover, the bottom friction is computed in KHIONE and not in TELEMAT-2D.

In most cases the undercover roughness of ice is not constant and may vary depending on many factors, one of which being the ice cover thickness. In KHIONE it is possible to increase linearly the roughness with the thickness of the ice cover with the keyword LAW FOR FRICTION COEFFICIENT = 1 (default = 0). The effective roughness coefficient becomes:

$$n_{ieff} = \frac{t_i n_i}{t_{ic}}, \quad (4.24)$$

with t_i the ice cover thickness (in m), t_{ic} the critical ice thickness (in m) which can be set with the keyword EQUIVALENT SURFACE ICE THICKNESS (default = 0.001). The range n_{ieff} is kept between the prescribed value of n_i and a value of n_{max} set with the keyword MAXIMAL FRICTION COEFFICIENT. This formula can only be used with a Manning friction law.

4.6.2 Ice cover thickness gradient source term

The weight of the ice cover leads to an increase of the pressure at the top of the water column. As a consequence, a moment source term is created which depends on the ice cover pressure gradient. The momentum source term due to the ice cover pressure, noted S_{pi} can be expressed as:

$$S_{pi} = -\frac{1}{\rho} \nabla p_i \quad (4.25)$$

in which p_i is the surface pressure increase due to the weight of the ice sheet. Supposing the ice cover density is constant, S_{pi} reads

$$S_{pi} = -g \frac{\rho_i}{\rho} \nabla t_i. \quad (4.26)$$

In KHIONE, this source term is either not taken into account or treated explicitly or implicitly depending on the value of the keyword MODEL FOR THE ICE COVER PRESSURE GRADIENT (default = 2):

- ▷ 0: no ice pressure gradient source term,
- ▷ 1: explicit ice pressure gradient source term,
- ▷ 2: implicit ice pressure gradient source term.

Note:

Only the explicit formulation is available when using the finite volume framework of TELEMAT-2D.

- [1] Wake A. and Rumer R.R. Effect of surface meltwater accumulation on the dissipation of lake ice. *Water Resource Research*, 15:430–434, 1979.
- [2] Ernest R Anderson. Energy-budget studies. *Water loss investigations: Lake Hefner studies. USGS Professional Paper*, 269:71–119, 1954.
- [3] A Andersson and LO Andersson. Frazil ice formation and adhesion on trash racks. In *Proc., Int. Association of Hydraulic Research Symp. on Ice, IAHR'92*, volume 2, pages 671–682, 1992.
- [4] Annika Andersson and Steven F Daly. Laboratory investigation of trash rack freezeup by frazil ice. Technical report, COLD REGIONS RESEARCH AND ENGINEERING LAB HANOVER NH, 1992.
- [5] George D Ashton. *River and lake ice engineering*. Water Resources Publication, 1986.
- [6] G. K. Batchelor. Mass transfer from small particles suspended in turbulent fluid. *Journal of Fluid Mechanics*, 98(3):609–623, 1980.
- [7] SJ Bolsenga. Total albedo of great lakes ice. *Water Resources Research*, 5(5):1132–1133, 1969.
- [8] Derek K Brady, Willard L Graves, and John Charles Geyer. Surface heat exchange at power plant cooling lakes. 1969.
- [9] T. Carstens. Experiments with supercooling and ice formation in flowing water. *Geofys. Publ. Norway*, 26(9)(3-18), 1966.
- [10] S. Clark and J Doering. Laboratory experiments on frazil-size characteristics in a counterrotating flume. *Journal of Hydraulic Engineering*, 132:94–101, 2006.
- [11] S. F. Daly. *Frazil ice dynamics*. CRREL Monograph 84-1, 1984.
- [12] S. F. Daly. Report on frazil ice. Technical report, International Association for Hydraulic Research, Working Group on Thermal Regimes, Special Report 94-23, 1994.
- [13] SF Daly. Modeling trash rack freezeup by frazil ice. In *Proc., 1st Int. Symp. on Cold Regions Heat Transfer*, pages 101–106. Edmonton Alberta, Canada, 1987.
- [14] Steven F Daly. Frazil ice blockage of intake trash racks. 1991.

- [15] Greene G.M. Simulation of ice-cover growth and decay in one-dimensional on the upper st. lawrence river. Technical Report NOAA Tech. Memo. ERL GLERL-36, Clarkson University, 1981.
- [16] John A Goff. Low-pressure properties of water-from 160 to 212° f. *Trans. Am. Heat. Vent. Eng.*, 52:95–121, 1946.
- [17] JP Gosink and TE Osterkamp. Measurements and analyses of velocity profiles and frazil ice-crystal rise velocities during periods of frazil-ice formation in rivers. *Annals of Glaciology*, 4:79–84, 1983.
- [18] P. Holland, D. L. Feltham, and S. F. Daly. On the nusselt number for frazil ice growth—a correction to “frazil evolution in channels” by lars hammar and hung-tao shen. *Journal of Hydraulic Research*, page pp. 1–4, 2006.
- [19] P. R. Holland and D. L. Feltham. Frazil dynamics and precipitation in a water column with depth-dependent supercooling. *Journal of Fluid Mechanics*, 530:101–124., 2005.
- [20] Fengbin Huang, Hung Tao Shen, and Ian Knack. Modeling border ice formation and cover progression in rivers. In *Proceedings of the 21st IAHR International Symposium on Ice, Dalian, China*, 2012.
- [21] Muhammad Iqbal. *An introduction to solar radiation*. Elsevier, 2012.
- [22] Ahintha Kandamby, Nimal Jayasundara, Hung Tao Shen, and Christoph Deyhle. A numerical river ice model for elbe river. In *20th IAHR International Symposium on Ice, Lahti, Finland*, 2010.
- [23] J. F. Kennedy, S. S. Lazier, B. Michel, and R. R. Jr. Rumer. Review of ice-hydraulic model studies. *Report to U.S. Army Engineering District, Detroit*, page 86p, 1981.
- [24] AM Wasantha Lal and Hung Tao Shen. Mathematical model for river ice processes. *Journal of hydraulic Engineering*, 117(7):851–867, 1991.
- [25] AMW Lal and HT Shen. A mathematical model for river ice processes (rice). *Report 89*, 4, 1989.
- [26] L Liu and HT Shen. A two-dimensional characteristic upwind finite element method for transitional open channel flow. *Report 03-04, Department of Civil and Environmental Engineering*, 2003.
- [27] Lianwu Liu, Hai Li, and Hung Tao Shen. A two-dimensional comprehensive river ice model. In *Proceedings of the 18th IAHR symposium on river ice, Sapporo, Japan*, volume 28, 2006.
- [28] V. MacFarlane, M. Loewen, and F. Hicks. Measurements of the size distribution of frazil ice particles in three alberta rivers. *Cold Regions Science and Technology*, 2017. doi: 10.1016/j.coldregions.2017.08.001.
- [29] V Matousek. Types of ice run and conditions for their formation. In *IAHR International Symposium on Ice*, volume 1, pages 315–327. Hamburg Germany, 1984.
- [30] V Matoušek. Frazil and skim ice formation in rivers. In *Proceedings of the IAHR Ice Symposium*, 1992.

- [31] Vaclav Matousek. Regularity of the freezing-up of the water surface and heat exchange between water body and water surface. In *IAHR Ice Symposium. Hamburg, Germany*, pages 187–201, 1984.
- [32] B Michel, N Marcotte, F Fonseca, and G Rivard. Formation of border ice in the st. anne river. In *Proceedings from the 2nd CRIPE Workshop. Edmonton, Alberta, Canada*, pages 38–61, 1982.
- [33] Brian Morse and Martin Richard. A field study of suspended frazil ice particles. *Cold Regions Science and Technology*, 55(1):86–102, 2009. doi: <https://doi.org/10.1016/j.coldregions.2008.03.004>.
- [34] A. Omstedt. Simulation of supercooling and size distribution in frazil ice dynamics. *Cold regions science and technology*, 1994.
- [35] Poothrikka P Paily, Enzo O Macagno, and John F Kennedy. Winter-regime thermal response of heated streams. *Journal of the Hydraulics Division*, 100(hy4), 1974.
- [36] D. W. Rees Jones and A. J. Wells. Frazil-ice growth rate and dynamics in mixed layers and sub-ice-shelf plumes. *The Cryosphere*, 12(1):25–38, 2018. doi: 10.5194/tc-12-25-2018.
- [37] Martin Richard and Brian Morse. Multiple frazil ice blockages at a water intake in the st. lawrence river. *Cold Regions Science and Technology*, 53(2):131–149, 2008.
- [38] VA Rimsha and RV Donchenko. The investigation of heat loss from free water surfaces in wintertime. *Leningrad Gosudarstvennyi Gidrologicheskii*, 64:58–83, 1957.
- [39] W Rodi. Turbulence models and their application in hydraulics-a state-of-the-art. *IAHR Publication, DELFT, The Netherlands*, 1980.
- [40] Donald R Satterlund. An improved equation for estimating long-wave radiation from the atmosphere. *Water Resources Research*, 15(6):1649–1650, 1979.
- [41] H. T. Shen and L. Hammar. Frazil evolution in channels. *Journal of Hydraulic Research*, 2010. doi: 10.1080/00221689509498572.
- [42] HT Shen and WA Van DeValk. Field investigation of st. lawrence river hanging ice dams. In *Proceedings, IAHR Ice Symposium*, pages 241–249, 1984.
- [43] Hung Tao Shen. Mathematical modeling of river ice processes. *Cold Regions Science and Technology*, 62(1):3–13, 2010.
- [44] Hung Tao Shen, De Sheng Wang, and AM Wasantha Lal. Numerical simulation of river ice processes. *Journal of Cold Regions Engineering*, 9(3):107–118, 1995.
- [45] Hung Tao Shen, Junshan Su, and Lianwu Liu. Sph simulation of river ice dynamics. *Journal of Computational Physics*, 165(2):752–770, 2000.
- [46] Chiang L.A. Shen H.T. Simulation of growth and decay of river ice cover. *Journal of Hydraulics Division*, 110:958–971, 1984.
- [47] P. H. Wadia. *Mass transfer from spheres and discs in turbulent agitated vessels*. PhD thesis, Department of Chemical Engineering, Massachusetts Institute of Technology, Cambridge, MA., 1974.